DMD Fast Forward. Published on January 20, 2020 as DOI: 10.1124/dmd.119.089656
This article has not been copyedited and formatted. The final version may differ from this version.

Quantitative Proteomics of Clinically Relevant Drug-Metabolizing Enzymes and Drug Transporters and Their Inter-correlations in the Human Small Intestine

Narciso Couto[1], Zubida M. Al-Majdoub[1], Stephanie Gibson[2], Pamela J. Davies[2], Brahim Achour[1], Matthew D. Harwood[3], Gordon Carlson[2], Jill Barber[1], Amin Rostami-Hodjegan[1,3], Geoffrey Warhurst[2]

1 Centre for Applied Pharmacokinetic Research, University of Manchester, Stopford Building, Oxford Road, Manchester, M13 9PT, UK.

2 Gut Barrier Group, Inflammation and Repair, University of Manchester, Salford Royal NHS Trust, Salford, M6 8HD, UK

3 Certara UK Limited (Simcyp Division), 1 Concourse Way, Sheffield, S1 2BJ, UK.

Running title: Quantification of DMEs and transporters in human intestine.

Correspondence to:

Narciso Couto and Amin Rostami-Hodjegan,

Centre for Applied Pharmacokinetic Research, University of Manchester, Stopford Building, Oxford Road, Manchester, M13 9PT, UK

Tel: +44 161 3060634

narciso.couto@manchester.ac.uk, ORCID ID: 0000-0001-7565-4357

amin.rostami@manchester.ac.uk, ORCID ID: 0000-0003-3917-844X

Downloaded from dmd.aspetjournals.org at ASPET Journals on April 19, 2024

DMD Fast Forward. Published on January 20, 2020 as DOI: 10.1124/dmd.119.089656
This article has not been copyedited and formatted. The final version may differ from this version.

Abbreviations

CYP, cytochrome P450; UGT, uridine 5'-diphosphate-glucuronosyltransferase; ABC, ATP-binding cassette; SLC, solute carrier; QconCAT, quantification concatemer; FASP, filter-aided sample preparation; LC-MS/MS, liquid chromatography-tandem mass spectrometry; MRM, multiple reaction monitoring; DMEs, drug-metabolizing enzymes; PBPK, physiologically-based pharmacokinetics.

Downloaded from dmd.aspetjournals.org at ASPET Journals on April 19, 2024

DMD Fast Forward. Published on January 20, 2020 as DOI: 10.1124/dmd.119.089656
This article has not been copyedited and formatted. The final version may differ from this version.

Abstract

The levels of drug metabolizing enzymes (DMEs) and transporter proteins in the human intestine are pertinent to determine oral drug bioavailability. Despite the paucity of reports on such measurements, it is well recognised that these values are essential for translating *in vitro* data on drug metabolism and transport to predict drug disposition in gut wall. In the current study, clinically relevant DMEs (cytochrome P450 (CYP) and uridine 5'-diphospho-glucuronosyltransferase (UGT)) and drug transporters were quantified in total mucosal protein preparations from the human jejunum (n = 4) and ileum (n = 12) using QconCAT-based targeted proteomics. In contrast to previous reports, UGT2B15 and OATP1A2 were quantifiable in *all* our samples. Overall, no significant disparities in protein expression were observed between jejunum and ileum. Relative mRNA expression for drug transporters did not correlate with the abundance of their cognate protein except for P-gp and OST-α, highlighting the limitations of RNA as a surrogate for protein expression in dynamic tissues with high turnover. Inter-correlations were found within CYP (2C9–2C19 (p = 0.002, R^2 = 0.63), 2C9–2J2 (p = 0.004, R^2 = 0.40), 2D6–2J2 (p = 0.002, R^2 = 0.50)) and UGT (1A1–2B7 (p = 0.02, R^2 = 0.87)) family of enzymes. There were also correlations between P-gp and several other proteins (OST-α (p < 0.0001, R^2 = 0.77), UGT1A6 (p = 0.009, R^2 = 0.38) and CYP3A4 (p = 0.007, R^2 = 0.30). Incorporating such correlations into building virtual populations is crucial for obtaining plausible characteristics of simulated individuals.

Downloaded from dmd.aspetjournals.org at ASPET Journals on April 19, 2024

DMD Fast Forward. Published on January 20, 2020 as DOI: 10.1124/dmd.119.089656
This article has not been copyedited and formatted. The final version may differ from this version.

Statement of Significance

A number of drug transporters were quantified for the first time in this study. Several inter-correlations of protein abundance were reported. mRNA expression levels proved to be a poor reflection of differences between individuals regarding the level of protein expression in gut. The reported abundance of DMEs and transporters and their inter-correlations will contribute to better predictions of oral drug bioavailability and drug–drug interactions by linking *in vitro* observations to potential outcomes through physiologically-based pharmacokinetic models.

Downloaded from dmd.aspetjournals.org at ASPET Journals on April 19, 2024

DMD Fast Forward. Published on January 20, 2020 as DOI: 10.1124/dmd.119.089656
This article has not been copyedited and formatted. The final version may differ from this version.

Introduction

Physiologically-based pharmacokinetic (PBPK) models are increasingly used to predict drug disposition, efficacy and toxicity across different patient populations. However, in order to achieve reliable information from PBPK models, they need to be populated with accurate experimental data where translation of *in vitro* data to anticipate *in vivo* observations is an essential element (Rostami-Hodjegan, 2012). Information regarding the abundance of drug-metabolizing enzymes (DMEs) and drug transporters in relevant human organs is crucial to building and refining PBPK models, consequently aiding the assessment of the performance of existing and new drugs in different patient populations and across different pathologies (Rostami-Hodjegan, 2012; Jamei, 2016).

The main organ responsible for drug metabolism in the human body is the liver; however, orally administered drugs need to cross the gastrointestinal tract, mainly through absorption in the small intestine, into the portal vein before arriving at the liver. The absorption of drugs from the small intestine is not only influenced by different families of DMEs such as cytochrome P450 (CYP) and uridine 5'-diphosphate-glucuronosyltransferase (UGT) but also by drug transporters from the ATP binding cassette (ABC) and solute carrier (SLC) families. However, the distribution of these enzymes and transporters may vary across different regions in the small intestine as these regions have distinct physiological roles. The physiologically variable and dynamic environment in the gut lumen together with high turnover of enterocytes (Darwich *et al.*, 2014, 2019) may play a role in the high interindividual variation observed in the abundance of these proteins (Paine, 2006). Thus, the prediction of the absorption and gut

Downloaded from dmd.aspetjournals.org at ASPET Journals on April 19, 2024

DMD Fast Forward. Published on January 20, 2020 as DOI: 10.1124/dmd.119.089656
This article has not been copyedited and formatted. The final version may differ from this version.

wall clearance of orally-administered drugs is considered to be difficult (Sjögren *et al.*, 2014). Therefore, in order to make meaningful progress towards achieving accurate PBPK predictions of absorption and gut wall clearance of orally administered drugs from the small intestine, it is vital that the abundance of DMEs and drug transporters and their variations are quantified in the small intestine. To capture the variability in a population, quantification of these protein abundances should be achieved in a sufficient number of individuals across different patient populations (Drozdzik *et al.*, 2018; Harwood *et al.*, 2019). The invasive nature of procedures and limited access to dedicated intestinal tissue banks has so far precluded such a large-scale study. Despite this challenge, published data do exist for DMEs and transporters in a relatively small number of samples (Gröer *et al.*, 2013; Sato *et al.*, 2014; Akazawa *et al.*, 2018; Harwood *et al.*, 2019). Regional variations in the abundance of some DMEs and drug transporters have been also reported in relatively few studies whilst no variations were observed in other studies (Drozdzik *et al.*, 2014, 2018). Challenges associated with obtaining intestinal tissue samples, increases the value of studies reporting the actual protein abundances as opposed to mRNA levels. There are a number of reports on mRNA expression data of genes encoding DMEs and drug transporters in the human small intestine (Thorn *et al.*, 2005; Clermont *et al.*, 2019; Fritz *et al.*, 2019)). However, caution should be exercised in using these values as the relationship between mRNA and protein abundance appears inconsistent (Berggren *et al.*, 2007; Hayeshi *et al.*, 2008) suggesting that mRNA data in a high turnover tissue such as intestine may have limited utility for PBPK modelling. In contrast, evidence of a good correlation between protein abundance and protein activity

Downloaded from dmd.aspetjournals.org at ASPET Journals on April 19, 2024

DMD Fast Forward. Published on January 20, 2020 as DOI: 10.1124/dmd.119.089656
This article has not been copyedited and formatted. The final version may differ from this version.

has recently been reported for DMEs and transporters (Achour *et al.*, 2017; Couto *et al.*, 2019; El-Khateeb *et al.*, 2019) in other organs such as liver. This suggests that the availability of abundance data for these proteins will be key to developing robust PBPK models for oral drug absorption.

Using QconCAT-based proteomics and a well-established proteomic workflow, we aimed to quantify the protein abundance of key CYP (2C9, 2C19, 2D6, 2J2 and 3A4) and UGT (1A1, 1A3, 1A6, 2B7 and 2B15) enzymes in two regions of the human small intestine, the jejunum and ileum. Simultaneously, several transporters from the SLC and ABC protein families (P-gp, BCRP, MRP2, OST-α, OST-β, OATP1A2 and OATP2B1) were also quantified. In addition, the mRNA expression levels of relevant transporters were measured in the same samples, enabling the assessment of correlations between mRNA expression and protein abundance of transporters. Due to the relatively large number of samples, in comparison with existent proteomics studies of DMEs and drug transporters in human intestine, inter-correlation between the protein abundance of enzymes and transporters was also investigated. The impact of factors such as age and sex on the expression of drug metabolising enzymes and transporters was also evaluated.

Materials and Methods

Chemicals

Unless otherwise indicated, all chemicals were supplied by Sigma-Aldrich (Poole, UK) with the highest purity available. All solvents were HPLC grade and supplied by ThermoFisher Scientific (Paisley, UK). Unlabelled peptide standard

Downloaded from dmd.aspetjournals.org at ASPET Journals on April 19, 2024

DMD Fast Forward. Published on January 20, 2020 as DOI: 10.1124/dmd.119.089656
This article has not been copyedited and formatted. The final version may differ from this version.

EGVNDNEEGFFSAR ([Glu[1]]-Fibrinopeptide B) and its modified analogue GVNDNEEGFFSAR, both with 95% purity were purchased from Severn Biotech Ltd. (Worcestershire, UK). Lysyl endopeptidase®, mass spectrometry grade, was purchased from Wako (Osaka, Japan). Sequencing grade modified trypsin was supplied by Promega (Southampton, UK). Complete Mini, EDTA-free protease inhibitor cocktail tablets were supplied by Roche (Mannheim, Germany). The DNA constructs for the QconCATs were produced by PolyQuant GmbH (http://www.polyquant.com/) (Rogensburg, Germany) using the expression vector pET21a encoding ampicillin and kanamycin resistance.

Human intestinal samples

Human intestinal tissues (16 donors) were obtained after informed consent from patients undergoing intestinal surgery at Salford Royal NHS Foundation Trust, Salford, UK. Prior ethics committee approval had been granted by the North West Research Ethics Committee, UK (06/1410/126), and all procedures were carried out in accordance with the Declaration of Helsinki guidelines. Samples were removed from the healthy margins of resected specimens at a minimum of 5 cm from the diseased mucosa and were macroscopically normal. Following removal of the intestinal sample, mucosal tissue was rapidly separated from muscle and serosal layers by blunt dissection. Samples of mucosa (~1 cm^2) were then snap frozen in liquid N_2 and stored at -80°C for subsequent analysis of protein abundance and mRNA expression. Donors demographic (ethnicity, age and gender) and clinical (medical history and medications) information are provided in Supplementary Information Table 1. An overview of the experimental workflow is shown in Supplementary Information Figure 1.

Downloaded from dmd.aspetjournals.org at ASPET Journals on April 19, 2024

DMD Fast Forward. Published on January 20, 2020 as DOI: 10.1124/dmd.119.089656
This article has not been copyedited and formatted. The final version may differ from this version.

Tissue preparation and isolation of total human mucosal protein

Snap-frozen mucosal tissue samples were ground to powder using a cooled mortar and pestle. This was resuspended in radioimmunoprecipitation assay (RIPA) lysis buffer containing 150 mM NaCl, 1% (v/v) Triton X-100, 0.5% (w/v) sodium deoxycholate, 0.1% (w/v) sodium dodecylsulfate (SDS), 50 mM Tris base pH 8.0. The buffer also contained protease inhibitors (0.5 mM phenylmethanesulfonylfluoride and 50 µL mL^{-1} protease inhibitor cocktail).Following incubation and mixing at 4°C for 30 min, the extract was centrifuged at 14,000 g for 5 minutes at 4°C. The supernatant was removed and stored in aliquots at -80°C. RIPA buffer was used for protein extraction as it has been shown to be a stringent lysis buffer capable of solubilising cellular membranes to enable quantification of proteins localized at the endoplasmic reticulum and plasma membrane (Padilla-Benavides *et al.*, 2010; Feng *et al.*, 2015). The use of RIPA buffer followed by centrifugation is not a membrane protein enrichment technique. Therefore, the protein samples extracted using this strategy is representative of total cellular protein.

QconCAT design and expression

Two different QconCATs previously designed to quantify human hepatic transporters (TransCAT) and human hepatic metabolizing enzymes (MetCAT) were used to quantify the same transporters and DMEs from human intestinal tissues (Russell *et al.*, 2013; Harwood *et al.*, 2015). From the MetCAT construct, two unique peptides belonging to each of five CYP450s (CYP2C9, CYP2C19, CYP2D6, CYP2J2 and CYP3A4) and five UGTs (UGT1A1, UGT1A3, UGT1A6, UGT2B7 and UGT2B15) were selected for quantification. To enable accurate quantification of the MetCAT, [Glu^1]-Fibrinopeptide B

Downloaded from dmd.aspetjournals.org at ASPET Journals on April 19, 2024

DMD Fast Forward. Published on January 20, 2020 as DOI: 10.1124/dmd.119.089656
This article has not been copyedited and formatted. The final version may differ from this version.

analogue (GVNNEEGFFSAR) omitting the N-terminal glutamate residue was incorporated in the sequence. The TransCAT construct was designed to incorporate two unique peptides each belonging to specific transporter proteins of the ATP-binding cassette (ABC) family, i.e. P-gp, BCRP and MRP2 and the solute carrier superfamily (SLC) OST-α, OST-β, OATP1A2 and OATP2B1. In addition, two plasma membrane marker proteins, Na^+/K^+-ATPase and human peptide transporter 1 (cadherin-17) were included in this construct. To enable quantification of the TransCAT, [Glu^1]-fibrinopeptide B peptide sequence (EGVNDNEEGFFSAR) was also incorporated in the TransCAT sequence. The peptides selected for quantification are shown in Supplementary Tables 2 and 3. Expression of heavy isotope labelled MetCAT and TransCAT in *E. coli* was carried out as previously described (Russell *et al.*, 2013).

Protein content quantification

Protein content of the human intestinal extracts was estimated using Bradford protein assay according to the manufacturer's instructions. This involved Bio-Rad based on the Coomassie brilliant blue G-250 dye (ThermoFisher Scientific, Hemel Hempstead, UK). Analysis was made in triplicate according to the manufacturer's protocol using bovine serum albumin (BSA) as a standard. To minimise the effect of RIPA buffer components on the determination of protein content in the total mucosal protein extracts, mucosal intestine samples were diluted 100 times in HPLC water, before the assay was performed.

RNA extraction and qRT-PCR

Downloaded from dmd.aspetjournals.org at ASPET Journals on April 19, 2024

DMD Fast Forward. Published on January 20, 2020 as DOI: 10.1124/dmd.119.089656
This article has not been copyedited and formatted. The final version may differ from this version.

Snap-frozen tissue samples were ground to powder and total RNA was extracted by re-suspending in Tri-Reagent (Thermo Fisher Scientific, Hemel Hempstead, UK) and processing using standard procedures. Following determination of the concentration and purity of isolated RNA by A_{260}/A_{280} spectrophotometry, cDNA was prepared from 3 µg total RNA in a total volume of 20 µL using the Roche Transcriptor First Strand cDNA Synthesis kit (Roche, Burgess Hill, UK).

Relative quantification of gene expression was undertaken for 7 transporters (ABCB1, ABCG2, ABCC2, SLCO2B1, SLC51A, SLC51B, CDH-17) by real-time PCR using the Roche Universal Probe Library system (UPL; Roche). Using the UPL Genefinder software, gene-specific intron-spanning primers and appropriate fluorescent hydrolysis probes were designed for each transporter. Assays were performed using the Roche Lightcycler 480 platform in a total volume of 20 µL with 200 nM forward and reverse primers; 100 nM of the UPL hydrolysis probe and ~0.3 µg cDNA. The ΔΔCT method was used to determine mRNA expression relative to reference genes glyceraldehyde 3-phosphate dehydrogenase (GAPDH) and villin 1 (VIL1). Sequences of the PCR primers are supplied in Supplementary Table 4

Total mucosal protein digestion

To enable quantification by mass spectrometry, 20 µg of each total mucosal protein fraction was spiked with a known amount of isotope-labelled MetCAT and TransCAT. To each fraction containing the MetCAT and TransCAT standards, sodium deoxycholate was added to a final concentration of 5% (w/v). The mixture was thoroughly mixed and incubated at room temperature for 10 minutes.

Downloaded from dmd.aspetjournals.org at ASPET Journals on April 19, 2024

DMD Fast Forward. Published on January 20, 2020 as DOI: 10.1124/dmd.119.089656
This article has not been copyedited and formatted. The final version may differ from this version.

For protein digestion, the filter-aided sample preparation (FASP) method (Wisniewski *et al.*,2009) was adopted as previously described (Al Feteisi *et al.*, 2018; Al-Majdoub *et al.*, 2019; Couto *et al.*, 2019). Briefly, the detergent-solubilized proteins from the human total mucosal protein samples were reduced using 100 mM 1,4-dithiothreitol (DTT), followed by alkylation with 50 mM iodoacetamide. After alkylation, deoxycholate removal was performed by buffer exchange using successive washes with 8 M urea in 100 mM Tris-HCl (pH 8.5). To reduce urea concentration, three additional washes were performed using 1 M urea in 50 mM ammonium bicarbonate (pH 8.5). Protein digestion was achieved by sequential treatment with endopeptidase Lys-C and trypsin (Al-Majdoub *et al.*, 2014). Firstly, Lys-C was added at an enzyme: protein ratio of 1:50 followed by incubation at 37ºC for 4 hours. After Lys-C, trypsin was added at a ratio 1:25 enzyme:protein followed by overnight incubation at 37°C. Peptides were recovered by centrifugation (14,000 *g,* 20 min) followed by elution using 0.5 M sodium chloride. Unlabelled peptide standard EGVNDNEEGFFSAR ([Glu[1]]-Fibrinopeptide B) and its modified analogue GVNDNEEGFFSAR, were added and desalted using a C18 column (Thermo). The peptide mixtures were lyophilized using a vacuum concentrator and stored at -20°C until mass spectrometric analysis.

Liquid chromatography and mass spectrometry

Proteins were quantified by mass spectrometry targeted proteomics based on a published protocol (Harwood *et al.*, 2015). For all analyte peptides and their isotope labelled internal QconCAT peptides, three mass transitions were selected (see Supplementary Tables 2 and 3). Multiple reaction monitoring (MRM) acquisition was applied for optimisation of

Downloaded from dmd.aspetjournals.org at ASPET Journals on April 19, 2024

DMD Fast Forward. Published on January 20, 2020 as DOI: 10.1124/dmd.119.089656
This article has not been copyedited and formatted. The final version may differ from this version.

transitions using a pooled sample. Each individual sample was injected in duplicate into the LC system.

Briefly, dried peptide samples were resuspended in loading buffer (HPLC grade water containing 5% (v/v) HPLC grade acetonitrile and 0.1 % (v/v) formic acid) to reach a concentration of 1 µg uL^{-1} and 1.0 µL of each sample was loaded on an UltiMate® 3000 rapid separation liquid chromatography (RSLC), (Dionex, Surrey, UK) coupled to an on-line QTRAP 6500 mass spectrometer (SCIEX, Warrington, UK). Peptides were reversed-phase separated on a PepMap™ RSLC C18 column (2 µm particles, 100 Å, 75 µm inner diameter, 50 cm length, Thermo Scientific, UK) preceded by a C18 PepMap100 µ-precolumn (5 µm, 100 Å, 5 µm inner diameter, 5 mm length, ThermoFisher Scientific, UK). A multi-step gradient was used from 4% to 40% buffer B (80% (v/v) acetonitrile with 0.1% (v/v) formic acid) for 60 minutes at a flow rate of 300 nL min^{-1}. The composition of buffer A was HPLC grade water containing 0.1 % (v/v) formic acid.

Assessment of CYP, UGT and transporters abundance

Protein/peptide quantification was performed using Skyline v4.0 (https://skyline.ms/project/ home/software/Skyline/begin.view) (MacLean *et al.*, 2010). For each peptide of interest, MRM transitions were optimised using a pooled sample in a single analytical run. Two unique peptides and three transitions were used for the quantification of all CYP450 and UGT enzymes, except CYP3A4, UGT1A6 and UGT2B7 which were quantified using a single peptide. From the UGT enzymes, isomeric sequences, such as VSVWLLR and ADVWLIR unique to UGT1A6 and UGT2B7, respectively, were not considered because of the overlapping retention time and

Downloaded from dmd.aspetjournals.org at ASPET Journals on April 19, 2024

DMD Fast Forward. Published on January 20, 2020 as DOI: 10.1124/dmd.119.089656
This article has not been copyedited and formatted. The final version may differ from this version.

interference of signal intensities. All transporters were quantified using a single peptide and three transitions, except OATP2B1 which was quantified using a single peptide and two transitions only. Single peptides were used for quantification because the elution profile of the second peptides (in the heavy and light versions) was not of adequate quality to be considered for quantification. The peptide sequences used for quantification are provided in Supplementary Information Tables 2 and 3. Representative examples of MRM co-elution profiles for all transporters are shown in Supplementary Information Figures 2 and 3. For each selected targeted peptide, concentration was calculated based on the mean of at least two mass transitions per peptide.

Statistical analysis

All statistical analysis of the data was performed using Microsoft Excel 2010 and GraphPad Prism® v7.03 (La Jolla, California, USA). Non-parametric statistics were used since a considerable proportion of the dataset did not follow normal distribution. The normality of data distribution was assessed using three tests: D'Agostino-Pearson, Shapiro-Wilk and Kolmogorov-Smirnov normality tests. All protein expression data were presented as means ± standard deviation, coefficient of variation (CV) as well as minimum and maximum. The Spearman rank-order correlation (Rs) test, with *t*-distribution of the *p*-values, was used to assess mRNA-protein correlation and inter-correlation between protein abundance levels. The level of scatter of data was evaluated by linear regression (R^2). Correlations were considered strong when the values correlated well (Rs > 0.60) with statistical significance *p*-value less than 0.05 and demonstrated limited scatter ($R^2 > 0.30$). Rs values between 0.5 – 0.6 with a *p*-value less than 0.05 were considered to

Downloaded from dmd.aspetjournals.org at ASPET Journals on April 19, 2024

DMD Fast Forward. Published on January 20, 2020 as DOI: 10.1124/dmd.119.089656
This article has not been copyedited and formatted. The final version may differ from this version.

represent a moderate correlation. The relationship between age and expression level was also assessed using these correlation tests. Sample differences were evaluated using the nonparametric Mann-Whitney *U*-test and Kolmogorov-Smirnov cumulative distribution test. The relationship between protein abundance levels and the expression covariates, sex and disease, was assessed using Mann-Whitney *U*-test and Kruskal-Wallis one-way analysis of variance.

Results

In this study, the MetCAT standard was used to measure the abundance of clinically relevant DMEs from the CYP450 family (CYP2C9, CYP2C19, CYP2D6, CYP2J2 and CYP3A4) and UGT family (UGT1A1, UGT1A3, UGT1A6, UGT2B7 and UGT2B15), across 16 human intestine samples, 4 from the jejunum and 12 from the ileum. In the same experiment, the TransCAT was used to measure protein abundance of a membrane marker (Na^+/K^+-ATPase), relevant drug transporters from the ABC (P-gp, BCRP and MRP2) and SLC (OST-α, OST-β, OATP1A2 and OATP2B1) families and cadherin-17, a cell adhesion molecule which also functions as a proton-dependent oligopeptide transporter in the human intestine (Dantzig *et al.*, 1994). In addition to measurement of protein abundance, the relative mRNA expression levels of P-gp (ABCB1), MRP2 (ABCC2), BCRP (ABCG2), OST-α (SLC51A), OST-β (SLC51B), OATP2B1 (SLCO2B1) and cadherin-17 (CDH-17) were measured. The experimental workflow is shown in Supplementary Information Figure 1.

Abundance of CYP and UGT enzymes in human intestinal samples

Downloaded from dmd.aspetjournals.org at ASPET Journals on April 19, 2024

DMD Fast Forward. Published on January 20, 2020 as DOI: 10.1124/dmd.119.089656
This article has not been copyedited and formatted. The final version may differ from this version.

Table 1 and Figure 1 summarize the abundance of CYP and UGT enzymes in 4 jejunum and 12 ileum samples. All targeted CYPs were expressed in both jejunum and ileum, following the rank order: CYP3A4 > CYP2D6 > CYP2C9 > CYP2C19 > CYP2J2, with CYP3A4 being the most abundant in both the jejunum and ileum and CYP2D6 the second most abundant, yet being one order of magnitude lower and relatively close to the abundances of CYP2C9, CYP2C19 and CYP2J2. A marginally higher expression of CYP2C9, CYP2D6, CYP2J2 and CYP3A4 were found in the jejunum compared to the ileum, whilst for CYP2C19 this relationship is reversed. With the exception of CYP2J2, the abundance of CYP enzymes is more heterogeneous in the ileal samples compared with the jejunum (Table 1). With the exception of CYP3A4 (Mann-Whitney *U*-test, $p = 0.03$), no statistically significant differences were observed between quantified CYP abundances in jejunum and ileum.

The quantified UGT abundance levels followed the rank order: UGT1A1 > UGT2B7 > UGT1A3 > UGT1A6 > UGT2B15 in both jejunum and ileum. UGT1A1 was the most abundant UGT protein followed by UGT2B7 and UGT1A3 (Table 1 and Figure 1B), UGT2B15 was the least abundant in both intestinal regions. To the best of our knowledge, this is the first report of UGT2B15 abundance quantification in the human small intestine (Miyauchi *et al.*, 2016). In general, the average protein abundance of all UGTs tended to show a trend towards higher expression in the jejunum than in ileum; however, no statistically significant differences were observed.

Protein abundance and mRNA transcript abundance of ABC and SLC transporters in human intestinal samples

Downloaded from dmd.aspetjournals.org at ASPET Journals on April 19, 2024

DMD Fast Forward. Published on January 20, 2020 as DOI: 10.1124/dmd.119.089656
This article has not been copyedited and formatted. The final version may differ from this version.

With respect to measured abundances of transporters (Table 2 and Figure 2A), ABC transporters followed the rank order MRP2 > P-gp >= BCRP in both jejunum and ileum. In the SLC family of transporters, OATP2B1 was the most abundant protein followed by OST-α, OST-β and OATP1A2. In previous targeted proteomic studies, quantifying OATP1A2 above limits of quantification was challenging in intestinal samples (Gröer *et al.*, 2013; Drozdzik *et al.*, 2014; Nakamura *et al.*, 2016). A recent meta-analysis assessing relative and absolute regional expression of transporters in the intestine highlighted the challenges for assigning OATP1A2 expression directly into PBPK models where a mechanistic intestinal model is described (Harwood *et al.*, 2019). In this study however, the abundance of OATP1A2 in all 16 samples was found to be above the limit of quantification at relatively similar levels to OST-α and OST-β. No statistically significant differences in protein abundance between jejunum and ileum were observed for any of the ABC and SLC transporters measured. The only proteins showing significant differences between the two regions were cadherin-17 and Na^+/K^+-ATPase. The abundance of both proteins was higher in jejunum with the difference considered significant for cadherin-17 (Mann-Whitney U-test, $p = 0.03$) and moderately significant for Na^+/K^+-ATPase (Mann-Whitney U-test, $p = 0.058$).

mRNA expression relative to the reference gene GAPDH was determined for all transporters with the exception of SLCO1A2 (OATP1A2) and ATP1A1 (Na^+/K^+-ATPase). Figure 2B summarizes transporter mRNA expression and protein abundance levels of the cell-cell adhesion/peptide transporter CDH-17 (cadherin-17), the ABC transporters (ABCB1 (P-gp), ABCC2 (MRP2) and ABCG2 (BCRP)) and solute carrier transporters

Downloaded from dmd.aspetjournals.org at ASPET Journals on April 19, 2024

DMD Fast Forward. Published on January 20, 2020 as DOI: 10.1124/dmd.119.089656
This article has not been copyedited and formatted. The final version may differ from this version.

(SLC51A (OST-α), SLC51B (OST-β) and SLCO2B1 (OATP2B1)) in jejunum and ileum for the 16 human intestinal samples. CDH-17 (cadherin-17) exhibited the highest values for protein abundance and mRNA expression in both jejunum and ileum. However, the overall rank order of mRNA expression is markedly different to that of protein abundance. No statistically significant differences were observed between mRNA expression levels in the jejunum and ileum.

Correlation between protein abundance of CYPs and UGTs

Pairwise correlation in protein abundance within CYPs, UGTs and between CYPs and UGTs was tested with the nonparametric Spearman rank test. As shown in Figure 3, strong, significant and positive correlations were found only between select pairs of CYPs such as CYP2C9 – CYP2C19, CYP2C9 – CYP2J2 and CYP2D6 – CYP2J2. While a moderate correlation was found between abundance of CYP2D6 – CYP3A4. Analysis of correlations between UGT abundances indicate that a strong, significant and positive correlation was only observed between UGT1A1 – UGT2B7 whilst a moderate correlation was found between UGT1A3 – UGT2B15. In addition, strong, significant and positive correlations were found between protein abundances of certain CYPs and UGTs (Figure 4). The abundance of CYP2C9 correlates well with the abundances of UGT1A1, UGT1A3, UGT2B7 and UGT2B15. CYP2C19 and CYP2J2 abundances also correlated well with UGT2B15. A moderate correlation was found between the abundance of CYP2D6 and UGT2B15. In general, CYP3A4 does not correlate with the abundance of any of quantified UGTs with the exception of UGT1A6 where a strong correlation was found (Figure 4).

Downloaded from dmd.aspetjournals.org at ASPET Journals on April 19, 2024

DMD Fast Forward. Published on January 20, 2020 as DOI: 10.1124/dmd.119.089656
This article has not been copyedited and formatted. The final version may differ from this version.

Correlation between protein abundance of transporters, CYPs and UGTs

Pairwise correlation in abundance within transporters and between transporters and DMEs was tested with the nonparametric Spearman rank test. A positive, strong and significant correlation was only observed between P-gp – OST-α (p<0.0001, R^2 = 0.77). The correlation between the abundance of transporters and DMEs were predominantly between P-gp – UGT1A6 (p=0.009, R^2 = 0.38) and MRP2 – UGT1A1 (p=0.01, R^2 = 0.30). A moderate correlation between transporters and CYPs was only observed for OATP1A2 – CYP2J2 (p=0.01, R^2 = 0.20). Strong correlation was observed between P-gp and CYP3A4 (p=0.007, R^2 = 0.30, n =15).

Correlation between protein and mRNA of the quantified transporters

Pairwise correlation between mRNA expression and protein abundance within transporters was tested with the nonparametric Spearman rank test. Significant correlations were observed for only two transporters ABCB1/P-gp and SLC51A /OST-α although the latter showed a high level of scattering between data points (Figure 5A). Similar data was obtained using a second reference gene VIL1 to determine relative mRNA expression (Fig 5B).

Covariates of expression of intestinal enzymes and transporters

Trends in protein expression of DMEs and transporters were assessed with reference to several demographic and clinical factors, including sex, age, and disease state of donors. Demographic and clinical information on donors is provided in Supplementary Table 1. There were no statistically significant differences in protein abundance of DMEs and

Downloaded from dmd.aspetjournals.org at ASPET Journals on April 19, 2024

DMD Fast Forward. Published on January 20, 2020 as DOI: 10.1124/dmd.119.089656
This article has not been copyedited and formatted. The final version may differ from this version.

transporters between male (n=12) and female (n=4) donors and very little difference between healthy donors (n=5) and those with inflammatory bowel disease (n=3), colon cancer (n=5) or ischemia (n=3). A weak correlation (R^2 < 0.25 for all targets) was observed between protein expression and age (17-80 years).

Discussion

Drug absorption across the gut wall is a complex process. Drug bioavailability depends on the physicochemical properties of the drug and formulation and the activity of DMEs and drug transporters in the intestine (Olivares-Morales *et al.*, 2015; Gao *et al.*, 2017; Cristofoletti *et al.*, 2018; Darwich *et al.*, 2019). Regional differences in relative expression of enzymes and transporters can therefore play a significant role in defining the amount of drug that enters systemic circulation unchanged (Harwood *et al.*, 2013; Drozdzik *et al.*, 2014). Using a highly sensitive mass spectrometry platform and targeted quantitative proteomics (QconCAT) on human intestinal tissue from two different regions, jejunum and ileum, the abundance of various DMEs and drug transporters was quantified. Relative mRNA expression of several transporters was also measured. Although it is acknowledged that the duodenum could be a significant absorptive site for certain high permeability drugs, duodenal tissues were not available for this study. Resection of duodenum is rare and the surgical team associated with this study do not undertake procedures in this intestinal region of the bowel. However, the analysis of the jejunum and ileum regions of the bowel undertaken in this study is relevant as PBPK models generally consider the jejunum or ileum as the reference site for drug absorption/active

Downloaded from dmd.aspetjournals.org at ASPET Journals on April 19, 2024

DMD Fast Forward. Published on January 20, 2020 as DOI: 10.1124/dmd.119.089656
This article has not been copyedited and formatted. The final version may differ from this version.

transport due to their larger surface area and mean drug residence time (Bolger *et al.*, 2009; Harwood *et al.*, 2013).

All targeted CYPs were expressed in both jejunum and ileum with CYP3A4 being the most abundant CYP as previously reported (Paine, 2006; Drozdzik *et al.*, 2018), indicating the primary importance of CYP3A4 in pre-systemic drug metabolism (Supplementary Table 5). In contrast with other studies, where CYP2D6 is frequently below the limit of quantification (Supplementary Table 5), CYP2D6 was quantified in all analyzed samples. In individuals with a poor metabolizer phenotype, the expression of this enzyme is known to be compromised (Dickinson *et al.*, 2007). In the absence of related genotype information, which was not possible to obtain due to ethical constraints for this study, our results may indicate that the donors in the present study were not “poor metabolizers” since CYP2D6 was quantified in all samples with little variability in the same range as CYP2C9, frequently reported as the second most abundant enzyme in intestine (Miyauchi *et al.*, 2016; Drozdzik *et al.*, 2018). Differences between reported abundances of DMEs can also be associated with inter-laboratory differences in sample preparation methodologies. For example, some studies used intestinal microsomal fractions from enterocytes, others used total membrane-enriched fractions and others used the entire crude mucosa containing other types of intestinal cells. Inter-laboratory differences in the proteomic workflow can also contribute to technical variability in reported values (Harbourt *et al.*, 2012; Harwood *et al.*, 2014; Sato *et al.*, 2014; Nakamura *et al.*, 2016; Akazawa *et al.*, 2018).

Downloaded from dmd.aspetjournals.org at ASPET Journals on April 19, 2024

DMD Fast Forward. Published on January 20, 2020 as DOI: 10.1124/dmd.119.089656
This article has not been copyedited and formatted. The final version may differ from this version.

UGT1A1 was the most abundant UGT followed by UGT2B7 and UGT1A3, which is partially in agreement with published literature (Harbourt *et al.*, 2012; Sato *et al.*, 2014; Miyauchi *et al.*, 2016; Nakamura *et al.*, 2016). The concentration of UGT1A6 was equal in jejunum and ileum. Notably, we quantified UGT2B15 in both regions in spite of its low concentration and challenges associated with quantifying this enzyme. So far UGT2B15 abundance has been reported in one individual within a population of 28 individuals (Miyauchi *et al.*, 2016). In agreement with published data, the low abundance of these enzymes highlights the relatively minor role of these UGTs in comparison with CYPs in intestinal drug clearance (Drozdzik *et al.*, 2018).

A study in which ileum and jejunum samples were examined from the same donors reported differences in DME abundances between ileum and jejunum (Drozdzik *et al.*, 2018). In our study, no significant differences were observed between the abundance of DMEs in jejunum and ileum, except in the case of CYP3A4. This may be because the ileum and jejunum samples were not obtained from the same donor and differences were obscured by high inter-individual variability and small number of jejunum samples analyzed.

In agreement with other studies, high intestinal abundances of Na^+/K^+-ATPase and cadherin-17 were quantified (Harwood *et al.*, 2015, 2016). This highlights the applicability of total mucosal protein fractions to quantify both microsomal-localized DMEs and plasma membrane marker proteins. MRP2 was found to be the most abundant ABC transporter while OATP2B1 was the most abundant SLC transporter. Conflicting reports are found in the literature with respect to the rank order of abundances of the transporters quantified

Downloaded from dmd.aspetjournals.org at ASPET Journals on April 19, 2024

in this study (Gröer *et al.*, 2013; Drozdzik *et al.*, 2014, 2019; Miyauchi *et al.*, 2016). This can be due to differences in sample preparation techniques, proteomic and inter-individual variability (Gröer *et al.*, 2013; Drozdzik *et al.*, 2014; Harwood *et al.*, 2014, 2016). Notably, we were able to quantify OATP1A2 which has not been detected in other studies (Hilgendorf *et al.*, 2007; Meier *et al.*, 2007; Drozdzik *et al.*, 2014). The presence of OATP1A2 in the intestine has been disputed, although it has been observed immunohistochemically and is implicated in intestinal drug interactions with fruit juice (Glaeser *et al.*, 2007; Tamai, 2012; Estudante *et al.*, 2013). The high selectivity and sensitivity of our methodology provides confidence in our ability to detect this protein in these samples. Similar quantitative values of OST-α and OST-β are reported in our study, which conforms to our understanding that these sub-units form a dimeric complex which is functionally expressed in the basal membrane of enterocytes (Seward *et al.*, 2003).

Inter-correlations in protein abundance between DMEs and/or drug transporters have recently started to be used in PBPK models with the aim of achieving biologically-plausible predictions of drug pharmacokinetics (Melillo *et al.*, 2019). For instance, in studies involving the human liver, the utility of accounting for the inter-correlation between CYP3A4 and CYP2C8 abundance has been demonstrated in predicting drug clearance and drug-drug interactions between repaglinide and gemfibrozil (Doki *et al.*, 2018). In a separate study involving human liver microsomes, strong inter-correlations have also been reported for several CYPs and UGTs, however their physiological relevance is unclear (Achour *et al.*, 2014). As the functional interplay between DMEs and drug transporters is increasingly explored, the analysis of protein abundance inter-correlations

Downloaded from dmd.aspetjournals.org at ASPET Journals on April 19, 2024

DMD Fast Forward. Published on January 20, 2020 as DOI: 10.1124/dmd.119.089656
This article has not been copyedited and formatted. The final version may differ from this version.

presents valuable data for model refinement. Inter-correlations were found between CYPs, between UGTs, between CYPs and UGTs, and between DMEs and transporters, in line with that previously established in studies using mRNA expression levels at the mRNA level, strong inter-correlations have been reported between CYP3A4–ABCB1 (P-gp) and UGT1A1–ABCC2 (MRP2) (Drozdzik *et al.*, 2014; Bruckmueller *et al.*, 2017; Fritz *et al.*, 2019). In the present study, similar strong inter-correlation was observed at the protein level between these protein pairs. It is known that CYP3A4 and P-gp work synergistically leading to an efficient first-pass drug extraction in the intestine (Cummins, 2002). There is also evidence associating the transmembrane transport of hydrophilic glucuronide metabolites formed by UGTs via MRP2 (Li *et al.*, 2019), therefore these correlations have some physiological basis. A strong correlation observed between the P-gp and OST-α abundances in the gut wall (R^2 = 0.77) is expected only if they are regulated by the same nuclear receptors and/or if they share a common regulatory pathway (Tanigawara *et al.*, 1999; Kast *et al.*, 2002; Luo, 2002; Trubetskoy *et al.*, 2005; Urquhart *et al.*, 2007). For many proteins studied here, the organ-specific regulatory mechanisms are likely to be complex and not consistently well characterized. In the present study, no significant correlation was observed between the P-gp and BCRP abundance despite a significant inter-correlation being found between their respective mRNA levels (p = 0.009, R^2 = 0.31). The presence or absence of correlations between mRNA and protein has previously been described and post-translational differences may play a role depending on age or disease-related protein modification and processing (Harwood *et al.*, 2016).

Downloaded from dmd.aspetjournals.org at ASPET Journals on April 19, 2024

DMD Fast Forward. Published on January 20, 2020 as DOI: 10.1124/dmd.119.089656
This article has not been copyedited and formatted. The final version may differ from this version.

There is growing body of evidence that mRNA expression is a poor surrogate for protein abundance in absence of steady-state conditions. This is relevant to the dynamic environment of the gut lumen. Environmental inducers (daily variations in food and beverages) and a high turnover of enterocytes (3.5 days (Darwich *et al.*, 2014)) are likely to make the expression of proteins in the gut epithelium a dynamic process, making steady state conditions unlikely, thus justifying the use of protein abundance in preference to mRNA in *in vitro* to *in vivo* extrapolation-PBPK models.

Various demographic covariates were assessed for their effects on protein abundance including gender and age. There was no significant relationship with protein expression levels in either region of the intestine. However, the value of the covariate analysis is limited due to the small sample size. Covariate analysis has not been undertaken before mainly due to the low number of samples used in previous studies (Oswald *et al.*, 2013; Drozdzik *et al.*, 2014; Harwood *et al.*, 2015). A more recent study (Miyauchi *et al.*, 2016) assessed the effects of sex, age, smoking, and obesity on the expression of enzymes and transporters in the jejunal membrane fractions from 28 morbidly obese donors, and there was an overall lack of effect of age or gender on expression. These observations are consistent with data from the liver, which showed limited differences due to gender and lack of correlation with age after maturity (Achour *et al.*, 2014; Prasad *et al.*, 2014; Couto *et al.*, 2019). The impact of drugs administered to individuals in this study should also be carefully considered. The proton pump inhibitor omeprazole, which is predominantly metabolized by CYP2C19, has been shown to downregulate CYP2C19

Downloaded from dmd.aspetjournals.org at ASPET Journals on April 19, 2024

DMD Fast Forward. Published on January 20, 2020 as DOI: 10.1124/dmd.119.089656
This article has not been copyedited and formatted. The final version may differ from this version.

expression (Zvyaga *et al.*, 2012). In our study, 7 out of 16 donors were administered omeprazole but no effect on CYP2C19 expression was observed.

It is intended that the data generated in this study will be incorporated into whole body PBPK models. However, the matrix in which the abundances of drug metabolising enzymes and drug transporters were measured require careful consideration and application of appropriate scaling factors before incorporation into the PBPK model. Ongoing efforts in our research group are focussed on developing appropriate scaling factors.

In conclusion, the present study provides an in-depth analysis of protein abundance and protein abundance inter-correlations between DMEs and transporters in the human jejunum and ileum. Various covariates of expression were examined and expression of pharmacologically active proteins was shown to be independent of gender and age. The use of quantitative measurements of protein abundance together with other physiological and drug-specific measurements can facilitate predictions of drug absorption and clearance in the human intestine. The data in this study contribute to a growing body of evidence reporting absolute enzyme and transporter abundances in the human intestine that can be incorporated into population-based PBPK models.

Downloaded from dmd.aspetjournals.org at ASPET Journals on April 19, 2024

DMD Fast Forward. Published on January 20, 2020 as DOI: 10.1124/dmd.119.089656
This article has not been copyedited and formatted. The final version may differ from this version.

Acknowledgements

The authors thank the Innovative Medicines Initiative Joint Undertaking (http://www.imi.europa.eu) under grant agreement n° 115369, resources of which are composed of financial contribution from the European Union's Seventh Framework Programme (FP7/2007-2013) and EFPIA companies' in kind contribution. The authors also thank the Royal Commission for the Exhibition of 1851 for their award to the University of Manchester on the basis of M.D. Harwood successfully completing an Industrial Fellowship grant in 2015 which facilitated the initial aspects of this work. The authors also thank the Bio-MS core facility, University of Manchester, for providing access to LC-MS instrumentation and assistance with method development. Authors would like to thank Dr Sibylle Neuhoff for constructive comments during preparation of this manuscript, and Eleanor Savill for helping to format and submit the manuscript.

Author contributions

Participated in research design: Harwood, Carlson, Rostami-Hodjegan, and Warhurst

Conducted experiments: Couto, Al-Majdoub, Achour, Harwood, Gibson, and Davies

Contributed new reagents or analytic tools: Couto, and Al-Majdoub

Performed data analysis: Couto, Al-Majdoub, Barber, and Achour

Wrote or contributed to the writing of the manuscript: All

Conflict of interests

Matthew Harwood and Amin Rostami-Hodjegan are employees of Certara UK Limited.

Downloaded from dmd.aspetjournals.org at ASPET Journals on April 19, 2024

DMD Fast Forward. Published on January 20, 2020 as DOI: 10.1124/dmd.119.089656
This article has not been copyedited and formatted. The final version may differ from this version.

Supporting material information

Supplementary information contains 6 Tables and 3 Figures. In Tables, information regarding demographic and clinical information for the intestinal tissue donors (Table 1), selected standard peptides (MetCAT and TransCAT) and MRM transition schedules (Tables 2 and 3), PCR primers (forward and reverse) for human intestinal transporters (Table 4), and the abundance of DMEs and drug transporters in human intestine from different studies (Tables 5 and 6) is shown. In Figure 1, a schematic representation of the experimental workflow used in this study is shown. In Figures 2 and 3, representative examples of MRMs profiles are represented.

Downloaded from dmd.aspetjournals.org at ASPET Journals on April 19, 2024

DMD Fast Forward. Published on January 20, 2020 as DOI: 10.1124/dmd.119.089656
This article has not been copyedited and formatted. The final version may differ from this version.

References

Achour B, Dantonio A, Niosi M, Novak JJ, Fallon JK, Barber J, Smith PC, Rostami-Hodjegan A, and Goosen TC (2017) Quantitative characterization of major hepatic UDP-glucuronosyltransferase enzymes in human liver microsomes: Comparison of two proteomic methods and correlation with catalytic activity. *Drug Metab Dispos* **45**:1102–1112.

Achour B, Russell MR, Barber J, and Rostami-Hodjegan A (2014) Simultaneous Quantification of the Abundance of Several Cytochrome P450 and Uridine 5'-Diphospho-Glucuronosyltransferase Enzymes in Human Liver Microsomes Using Multiplexed Targeted Proteomics. *Drug Metab Dispos* **42**:500–510.

Akazawa T, Uchida Y, Miyauchi E, Tachikawa M, Ohtsuki S, and Terasaki T (2018) High Expression of UGT1A1/1A6 in Monkey Small Intestine: Comparison of Protein Expression Levels of Cytochromes P450, UDP-Glucuronosyltransferases, and Transporters in Small Intestine of Cynomolgus Monkey and Human. *Mol Pharm* **15**:127–140.

Al-Majdoub ZM, Al Feteisi H, Achour B, Warwood S, Neuhoff S, Rostami-Hodjegan A, and Barber J (2019) Proteomic Quantification of Human Blood-Brain Barrier SLC and ABC Transporters in Healthy Individuals and Dementia Patients. *Mol Pharm* **16**:1220–1233.

Al-Majdoub ZM, Carroll KM, Gaskell SJ, and Barber J (2014) Quantification of the proteins

Downloaded from dmd.aspetjournals.org at ASPET Journals on April 19, 2024

of the bacterial ribosome using QconCAT technology. *Journal Proteome Res* **13**:1211–1222.

Al Feteisi H, Al-Majdoub ZM, Achour B, Couto N, Rostami-Hodjegan A, and Barber J (2018) Identification and quantification of blood-brain barrier transporters in isolated rat brain microvessels. *J Neurochem* **146**:670–685.

Berggren S, Gall C, Wollnitz N, Ekelund M, Karlbom U, Hoogstraate J, Schrenk D, and Lennernäs H (2007) Gene and Protein Expression of P-Glycoprotein, MRP1, MRP2, and CYP3A4 in the Small and Large Human Intestine. *Mol Pharm* **4**:252–257.

Bolger MB, Lukacova V, and Woltosz WS (2009) Simulations of the Nonlinear Dose Dependence for Substrates of Influx and Efflux Transporters in the Human Intestine. *AAPS J* **11**:353–363.

Bruckmueller H, Martin P, Kähler M, Haenisch S, Ostrowski M, Drozdzik M, Siegmund W, Cascorbi I, and Oswald S (2017) Clinically Relevant Multidrug Transporters Are Regulated by microRNAs along the Human Intestine. *Mol Pharm* **14**:2245–2253.

Clermont V, Grangeon A, Barama A, Turgeon J, Lallier M, Malaise J, and Michaud V (2019) Activity and mRNA expression levels of selected cytochromes P450 in various sections of the human small intestine. *Br J Clin Pharmacol* **85**:1367–1377.

Couto N, Al-Majdoub ZM, Achour B, Wright PC, Rostami-Hodjegan A, and Barber J (2019) Quantification of Proteins Involved in Drug Metabolism and Disposition in the

Downloaded from dmd.aspetjournals.org at ASPET Journals on April 19, 2024

DMD Fast Forward. Published on January 20, 2020 as DOI: 10.1124/dmd.119.089656
This article has not been copyedited and formatted. The final version may differ from this version.

Human Liver Using Label-Free Global Proteomics. *Mol Pharm* **16**:632–647.

Cristofoletti R, Rowland M, Lesko LJ, Blume H, Rostami-Hodjegan A, and Dressman JB (2018) Past, Present, and Future of Bioequivalence: Improving Assessment and Extrapolation of Therapeutic Equivalence for Oral Drug Products. *J Pharm Sci* **107**:2519-2530.

Cummins CL (2002) Unmasking the Dynamic Interplay between Intestinal P-Glycoprotein and CYP3A4. *J Pharmacol Exp Ther* **300**:1036–1045.

Dantzig A, Hoskins J, Tabas L, Bright S, Shepard R, Jenkins I, Duckworth D, Sportsman, Mackensen D, Rosteck P, and Et A (1994) Association of intestinal peptide transport with a protein related to the cadherin superfamily. *Science* **264**:430–433.

Darwich AS, Aslam U, Ashcroft DM, and Rostami-Hodjegan A (2014) Meta-Analysis of the Turnover of Intestinal Epithelia in Preclinical Animal Species and Humans. *Drug Metab Dispos* **42**:2016–2022.

Darwich AS, Burt HJ, and Rostami-Hodjegan A (2019) The nested enzyme-within-enterocyte (NEWE) turnover model for predicting dynamic drug and disease effects on the gut wall. *Eur J Pharm Sci* **131**:195–207.

Dickinson GL, Rezaee S, Proctor NJ, Lennard MS, Tucker GT, and Rostami-Hodjegan A (2007) Incorporating In Vitro Information on Drug Metabolism Into Clinical Trial Simulations to Assess the Effect of CYP2D6 Polymorphism on Pharmacokinetics and

Downloaded from dmd.aspetjournals.org at ASPET Journals on April 19, 2024

DMD Fast Forward. Published on January 20, 2020 as DOI: 10.1124/dmd.119.089656
This article has not been copyedited and formatted. The final version may differ from this version.

Pharmacodynamics: Dextromethorphan as a Model Application. *J Clin Pharmacol* **47**:175–186.

Doki K, Darwich AS, Achour B, Tornio A, Backman JT, and Rostami-Hodjegan A (2018) Implications of intercorrelation between hepatic CYP3A4-CYP2C8 enzymes for the evaluation of drug-drug interactions: a case study with repaglinide. *Br J Clin Pharmacol* **84**:972–986.

Drozdzik M, Busch D, Lapczuk J, Janett M, Kurzawski M, and Oswald S (2018) Protein Abundance of Clinically Relevant Drug- Metabolizing Enzymes in the Human Liver and Intestine : A Comparative Analysis in Paired Tissue Specimens. *Clin Pharmacol Ther* **104**:515–524.

Drozdzik M, Busch D, Lapczuk J, Müller J, Ostrowski M, Kurzawski M, and Oswald S (2019) Protein Abundance of Clinically Relevant Drug Transporters in the Human Liver and Intestine: A Comparative Analysis in Paired Tissue Specimens. *Clin Pharmacol Ther* **105**:1204–1212.

Drozdzik M, Gröer C, Penski J, Lapczuk J, Ostrowski M, Lai Y, Prasad B, Unadkat JD, Siegmund W, and Oswald S (2014) Protein Abundance of Clinically Relevant Multidrug Transporters along the Entire Length of the Human Intestine. *Mol Pharm* **11**:3547–3555.

El-Khateeb E, Vasilogianni A-M, Alrubia S, Al-Majdoub ZM, Couto N, Howard M, Barber J, Rostami-Hodjegan A, and Achour B (2019) Quantitative mass spectrometry-based

Downloaded from dmd.aspetjournals.org at ASPET Journals on April 19, 2024

DMD Fast Forward. Published on January 20, 2020 as DOI: 10.1124/dmd.119.089656
This article has not been copyedited and formatted. The final version may differ from this version.

proteomics in the era of model-informed drug development: Applications in translational pharmacology and recommendations for best practice. *Pharmacol Ther* **Epub Ahead of Print**:107397.

Estudante M, Morais JG, Soveral G, and Benet LZ (2013) Intestinal drug transporters: An overview. *Adv Drug Deliv Rev* **65**:1340–1356.

Feng R, Ye J, Zhou C, Qi L, Fu Z, Yan B, Liang Z, Li R, and Zhai W (2015) Calreticulin down-regulation inhibits the cell growth, invasion and cell cycle progression of human hepatocellular carcinoma cells. *Diagn Pathol* **10**:149.

Fritz A, Busch D, Lapczuk J, Ostrowski M, Drozdzik M, and Oswald S (2019) Expression of clinically relevant drug-metabolizing enzymes along the human intestine and their correlation to drug transporters and nuclear receptors: An intra-subject analysis. *Basic Clin Pharmacol Toxicol* **124**:245–255.

Gao Y, Gesenberg C, and Zheng W (2017) Oral Formulations for Preclinical Studies, in *Developing Solid Oral Dosage Forms* (Qiu Y, Zhang GGZ, Mantri RV, Chen Y, Yu L eds) pp 455–495, 2nd ed, Elsevier.

Glaeser H, Bailey DG, Dresser GK, Gregor JC, Schwarz UI, McGrath JS, Jolicoeur E, Lee W, Leake BF, Tirona RG, and Kim RB (2007) Intestinal Drug Transporter Expression and the Impact of Grapefruit Juice in Humans. *Clin Pharmacol Ther* **81**:362–370.

Downloaded from dmd.aspetjournals.org at ASPET Journals on April 19, 2024

DMD Fast Forward. Published on January 20, 2020 as DOI: 10.1124/dmd.119.089656
This article has not been copyedited and formatted. The final version may differ from this version.

Gröer C, Brück S, Lai Y, Paulick A, Busemann A, Heidecke CD, Siegmund W, and Oswald S (2013) LC–MS/MS-based quantification of clinically relevant intestinal uptake and efflux transporter proteins. *J Pharm Biomed Anal* **85**:253–261.

Harbourt DE, Fallon JK, Ito S, Baba T, Ritter JK, Glish GL, and Smith PC (2012) Quantification of Human Uridine-Diphosphate Glucuronosyl Transferase 1A Isoforms in Liver, Intestine, and Kidney Using Nanobore Liquid Chromatography–Tandem Mass Spectrometry. *Anal Chem* **84**:98–105.

Harwood MD, Achour B, Neuhoff S, Russell MR, Carlson G, Warhurst G, and Rostami-Hodjegan A (2016) In Vitro-In Vivo Extrapolation Scaling Factors for Intestinal P-glycoprotein and Breast Cancer Resistance Protein: Part II. The Impact of Cross-Laboratory Variations of Intestinal Transporter Relative Expression Factors on Predicted Drug Disposition. *Drug Metab Dispos* **44**:476–480.

Harwood MD, Achour B, Russell MR, Carlson GL, Warhurst G, and Rostami-Hodjegan A (2015) Application of an LC–MS/MS method for the simultaneous quantification of human intestinal transporter proteins absolute abundance using a QconCAT technique. *J Pharm Biomed Anal* **110**:27–33.

Harwood MD, Neuhoff S, Carlson GL, Warhurst G, and Rostami-Hodjegan A (2013) Absolute abundance and function of intestinal drug transporters: a prerequisite for fully mechanistic in vitro-in vivo extrapolation of oral drug absorption. *Biopharm Drug Dispos* **34**:2–28.

Downloaded from dmd.aspetjournals.org at ASPET Journals on April 19, 2024

DMD Fast Forward. Published on January 20, 2020 as DOI: 10.1124/dmd.119.089656
This article has not been copyedited and formatted. The final version may differ from this version.

Harwood MD, Russell MR, Neuhoff S, Warhurst G, and Rostami-Hodjegan A (2014) Lost in Centrifugation! Accounting for Transporter Protein Losses in Quantitative Targeted Absolute Proteomics (QTAP). *Drug Metab Dispos* **42**:1766–1772.

Harwood MD, Zhang M, Pathak SM, and Neuhoff S (2019) The Regional-Specific Relative and Absolute Expression of Gut Transporters in Adult Caucasians: A Meta-Analysis. *Drug Metab Dispos* **47**:854–864.

Hayeshi R, Hilgendorf C, Artursson P, Augustijns P, Brodin B, Dehertogh P, Fisher K, Fossati L, Hovenkamp E, Korjamo T, Masungi C, Maubon N, Mols R, Müllertz A, Mönkkönen J, O'Driscoll C, Oppers-Tiemissen HM, Ragnarsson EGE, Rooseboom M, and Ungell A-L (2008) Comparison of drug transporter gene expression and functionality in Caco-2 cells from 10 different laboratories. *Eur J Pharm Sci* **35**:383–396.

Hilgendorf C, Ahlin G, Seithel A, Artursson P, Ungell A-L, and Karlsson J (2007) Expression of Thirty-six Drug Transporter Genes in Human Intestine, Liver, Kidney, and Organotypic Cell Lines. *Drug Metab Dispos* **35**:1333–1340.

Jamei M (2016) Recent Advances in Development and Application of Physiologically-Based Pharmacokinetic (PBPK) Models: a Transition from Academic Curiosity to Regulatory Acceptance. *Curr Pharmacol Reports* **2**:161–169.

Kast HR, Goodwin B, Tarr PT, Jones SA, Anisfeld AM, Stoltz CM, Tontonoz P, Kliewer S, Willson TM, and Edwards PA (2002) Regulation of Multidrug Resistance-

Downloaded from dmd.aspetjournals.org at ASPET Journals on April 19, 2024

DMD Fast Forward. Published on January 20, 2020 as DOI: 10.1124/dmd.119.089656
This article has not been copyedited and formatted. The final version may differ from this version.

associated Protein 2 (ABCC2) by the Nuclear Receptors Pregnane X Receptor, Farnesoid X-activated Receptor, and Constitutive Androstane Receptor. *J Biol Chem* **277**:2908–2915.

Li CY, Basit A, Gupta A, Gáborik Z, Kis E, and Prasad B (2019) Major glucuronide metabolites of testosterone are primarily transported by MRP2 and MRP3 in human liver, intestine and kidney. *J Steroid Biochem Mol Biol* **191**:105350.

Luo G (2002) CYP3A4 Induction by Drugs: Correlation between a Pregnane X Receptor Reporter Gene Assay and CYP3A4 Expression in Human Hepatocytes. *Drug Metab Dispos* **30**:795–804.

MacLean B, Tomazela DM, Shulman N, Chambers M, Finney GL, Frewen B, Kern R, Tabb DL, Liebler DC, and MacCoss MJ (2010) Skyline: an open source document editor for creating and analyzing targeted proteomics experiments. *Bioinformatics* **26**:966–968.

Meier Y, Eloranta JJ, Darimont J, Ismair MG, Hiller C, Fried M, Kullak-Ublick GA, and Vavricka SR (2007) Regional Distribution of Solute Carrier mRNA Expression Along the Human Intestinal Tract. *Drug Metab Dispos* **35**:590–594.

Melillo N, Darwich AS, Magni P, and Rostami-Hodjegan A (2019) Accounting for inter-correlation between enzyme abundance: a simulation study to assess implications on global sensitivity analysis within physiologically-based pharmacokinetics. *J Pharmacokinet Pharmacodyn* **46**:137–154.

Downloaded from dmd.aspetjournals.org at ASPET Journals on April 19, 2024

DMD Fast Forward. Published on January 20, 2020 as DOI: 10.1124/dmd.119.089656
This article has not been copyedited and formatted. The final version may differ from this version.

Miyauchi E, Tachikawa M, Declèves X, Uchida Y, Bouillot J-L, Poitou C, Oppert J-M, Mouly S, Bergmann J-F, Terasaki T, Scherrmann J-M, and Lloret-Linares C (2016) Quantitative Atlas of Cytochrome P450, UDP-Glucuronosyltransferase, and Transporter Proteins in Jejunum of Morbidly Obese Subjects. *Mol Pharm* **13**:2631–2640.

Nakamura K, Hirayama-Kurogi M, Ito S, Kuno T, Yoneyama T, Obuchi W, Terasaki T, and Ohtsuki S (2016) Large-scale multiplex absolute protein quantification of drug-metabolizing enzymes and transporters in human intestine, liver, and kidney microsomes by SWATH-MS: Comparison with MRM/SRM and HR-MRM/PRM. *Proteomics* **16**:2106–2117.

Olivares-Morales A, Lennernäs H, Aarons L, and Rostami-Hodjegan A (2015) Translating Human Effective Jejunal Intestinal Permeability to Surface-Dependent Intrinsic Permeability: a Pragmatic Method for a More Mechanistic Prediction of Regional Oral Drug Absorption. *AAPS J* **17**:1177–1192.

Oswald S, Gröer C, Drozdzik M, and Siegmund W (2013) Mass Spectrometry-Based Targeted Proteomics as a Tool to Elucidate the Expression and Function of Intestinal Drug Transporters. *AAPS J* **15**:1128–1140.

Padilla-Benavides T, Roldán ML, Larre I, Flores-Benitez D, Villegas-Sepúlveda N, Contreras RG, Cereijido M, and Shoshani L (2010) The Polarized Distribution of Na + ,K + -ATPase: Role of the Interaction between β Subunits. *Mol Biol Cell* **21**:2217–

Downloaded from dmd.aspetjournals.org at ASPET Journals on April 19, 2024

DMD Fast Forward. Published on January 20, 2020 as DOI: 10.1124/dmd.119.089656
This article has not been copyedited and formatted. The final version may differ from this version.

2225.

Paine MF (2006) THE HUMAN INTESTINAL CYTOCHROME P450 “PIE.” *Drug Metab Dispos* **34**:880–886.

Prasad B, Evers R, Gupta A, Hop CECA, Salphati L, Shukla S, Ambudkar S V., and Unadkat JD (2014) Interindividual variability in hepatic organic anion-transporting polypeptides and P-glycoprotein (ABCB1) protein expression: Quantification by liquid chromatography tandem mass spectroscopy and influence of genotype, age, and sex. *Drug Metab Dispos* **42**:78–88.

Rostami-Hodjegan A (2012) Physiologically Based Pharmacokinetics Joined With In Vitro–In Vivo Extrapolation of ADME: A Marriage Under the Arch of Systems Pharmacology. *Clin Pharmacol Ther* **92**:50–61.

Rostami-Hodjegan A, and Tucker GT (2007) Simulation and prediction of in vivo drug metabolism in human populations from in vitro data. *Nature Rev Drug Discov* **6**:140–148.

Russell MR, Achour B, McKenzie EA, Lopez R, Harwood MD, Rostami-Hodjegan A, and Barber J (2013) Alternative fusion protein strategies to express recalcitrant QconCAT proteins for quantitative proteomics of human drug metabolizing enzymes and transporters. *Journal Proteome Res* **12**:5934–5942.

Sato Y, Nagata M, Tetsuka K, Tamura K, Miyashita A, Kawamura A, and Usui T (2014)

Downloaded from dmd.aspetjournals.org at ASPET Journals on April 19, 2024

DMD Fast Forward. Published on January 20, 2020 as DOI: 10.1124/dmd.119.089656
This article has not been copyedited and formatted. The final version may differ from this version.

Optimized Methods for Targeted Peptide-Based Quantification of Human Uridine 5'-Diphosphate-Glucuronosyltransferases in Biological Specimens Using Liquid Chromatography-Tandem Mass Spectrometry. *Drug Metab Dispos* **42**:885–889.

Seward DJ, Koh AS, Boyer JL, and Ballatori N (2003) Functional complementation between a novel mammalian polygenic transport complex and an evolutionarily ancient organic solute transporter, OSTα-OSTβ. *J Biol Chem* **278:**27473-27482.

Sjögren E, Abrahamsson B, Augustijns P, Becker D, Bolger MB, Brewster M, Brouwers J, Flanagan T, Harwood M, Heinen C, Holm R, Juretschke H-P, Kubbinga M, Lindahl A, Lukacova V, Münster U, Neuhoff S, Nguyen MA, Peer A Van, Reppas C, Hodjegan AR, Tannergren C, Weitschies W, Wilson C, Zane P, Lennernäs H, and Langguth P (2014) In vivo methods for drug absorption – Comparative physiologies, model selection, correlations with in vitro methods (IVIVC), and applications for formulation/API/excipient characterization including food effects. *Eur J Pharm Sci* **57**:99–151.

Tamai I (2012) Oral drug delivery utilizing intestinal OATP transporters. *Adv Drug Deliv Rev* **64**:508–514.

Tanigawara Y, Aoyama N, Kita T, Shirakawa K, Komada F, Kasuga M, and Okumura K (1999) CYP2C19 genotype-related efficacy of omeprazole for the treatment of infection caused by Helicobacter pylori. *Clin Pharmacol Ther* **66:**528-534.

Thorn M, Finnstrom N, Lundgren S, Rane A, and Loof L (2005) Cytochromes P450 and

Downloaded from dmd.aspetjournals.org at ASPET Journals on April 19, 2024

DMD Fast Forward. Published on January 20, 2020 as DOI: 10.1124/dmd.119.089656
This article has not been copyedited and formatted. The final version may differ from this version.

MDR1 mRNA expression along the human gastrointestinal tract. *Br J Clin Pharmacol* **60**:54–60.

Trubetskoy O, Marks B, Zielinski T, Yueh M-F, and Raucy J (2005) A simultaneous assessment of CYP3A4 metabolism and induction in the DPX-2 cell line. *AAPS J* **7**:E6–E13.

Urquhart BL, Tirona RG, and Kim RB (2007) Nuclear Receptors and the Regulation of Drug-Metabolizing Enzymes and Drug Transporters: Implications for Interindividual Variability in Response to Drugs. *J Clin Pharmacol* **47**:566–578.

Wisniewski JR, Zougman A, Nagaraj N, Mann M, and Wi JR (2009) Universal sample preparation method for proteome analysis. *Nature Methods* **6:**359-362.

Zvyaga T, Chang S-Y, Chen C, Yang Z, Vuppugalla R, Hurley J, Thorndike D, Wagner A, Chimalakonda A, and Rodrigues AD (2012) Evaluation of Six Proton Pump Inhibitors As Inhibitors of Various Human Cytochromes P450: Focus on Cytochrome P450 2C19. *Drug Metab Dispos* **40**:1698–1711.

Downloaded from dmd.aspetjournals.org at ASPET Journals on April 19, 2024

DMD Fast Forward. Published on January 20, 2020 as DOI: 10.1124/dmd.119.089656
This article has not been copyedited and formatted. The final version may differ from this version.

Figure legends

Figure 1 – Abundance of drug-metabolizing enzymes in the human intestine. In panels A and B, scatter plots represent the abundance of drug-metabolizing CYP and UGT enzymes, respectively, in 16 human intestinal samples from jejunum (n=4) and ileum (n=12). Protein abundances are expressed as pmol mg^{-1} of total mucosal protein from intestinal tissue. Bars in black represent the mean.

Figure 2 – Quantification of protein abundance and mRNA expression of drug transporters in the human intestine. In panel A, scatter plots represent the protein abundance of relevant drug transporters from the ABC and SLC families as well as the plasma membrane markers Na^+/K^+-ATPase and cadherin-17 in 16 human intestinal tissue samples from jejunum and ileum. Protein abundances are expressed as pmol mg^{-1} of total mucosal protein from intestinal tissue. In panel B, scatter plots represent relative mRNA expression of selected drug transporters and the plasma membrane marker CDH-17 normalized to mRNA transcript levels of GAPDH in human intestinal tissue. RNA data were not collected for the gene ATP1A1 (corresponding to the protein Na^+/K-ATPase) and gene SLCO1A2 (protein OATP1A2). Proteins are denoted with their most common names and transcripts are denoted by their corresponding gene names. The protein cadherin-17 corresponds to CDH-17, P-gp corresponds to ABCB1, MRP2 corresponds to ABCC2, BCRP corresponds to ABCG2, OST-α and OST-β corresponds to SLC51A and SLC51B, respectively, and OATP2B1 corresponds to SLCO2B1. Bars in black represent the mean.

Downloaded from dmd.aspetjournals.org at ASPET Journals on April 19, 2024

DMD Fast Forward. Published on January 20, 2020 as DOI: 10.1124/dmd.119.089656
This article has not been copyedited and formatted. The final version may differ from this version.

Figure 3 – Observed significant correlations in protein abundances between CYPs (panel A) and between UGTs (panel B). Correlation analysis was performed using Spearman rank order correlation (Rs) test with *t*-distribution of the *p*-value. Linear regression analysis was carried out to assess the linearity of relationships and scatter of the data (R^2). Correlations were deemed strong when the Rs values were greater than 0.60, *p*-value less than 0.05 and the data points demonstrated limited scatter ($R^2 > 0.30$). Rs values between 0.5 – 0.6 with a *p*-value less than 0.05 were considered to represent moderate correlation. Clear circles with green border correspond to protein abundance in the ileum and clear circles with red border correspond to protein abundance in the jejunum.

Figure 4 – Observed correlations in protein abundances between CYP and UGT enzymes. Correlation analysis was performed using Spearman rank order correlation (Rs) test with *t*-distribution of the *p*-value. Linear regression analysis was carried out to assess the linearity of relationships and scatter of the data (R^2). Correlations were deemed strong when the Rs values were greater than 0.60, *p*-value less than 0.05 and the data points demonstrated limited scatter ($R^2 > 0.30$). Rs values between 0.5 – 0.6 with a *p*-value less than 0.05 were considered to represent moderate correlation. Clear circles with green border correspond to protein abundance in the ileum and clear circles with red border correspond to protein abundance in the jejunum.

Figure 5 – Observed correlations between transporter protein abundance and relative mRNA expression levels. In panel A, the x-axis represents mRNA expression levels of transporters normalised to mRNA expression levels of GAPDH and y-axis represents

Downloaded from dmd.aspetjournals.org at ASPET Journals on April 19, 2024

DMD Fast Forward. Published on January 20, 2020 as DOI: 10.1124/dmd.119.089656
This article has not been copyedited and formatted. The final version may differ from this version.

protein abundance. In panel B, the x-axis represents mRNA expression levels of transporters normalised to mRNA expression levels of villin 1 and y-axis represents protein abundance. Correlation analysis was assessed using Spearman rank order correlation (Rs) test with *t*-distribution of the *p*-value. Linear regression analysis was carried out to assess the linearity of relationships and scatter of the data (R^2). Correlations were deemed strong when the Rs values were greater than 0.60, *p*-value less than 0.05 and the data points demonstrated limited scatter ($R^2 > 0.30$). Rs values between 0.5 – 0.6 with a *p*-value less than 0.05 were considered to represent moderate correlation. Clear circles with green border correspond to ileal samples and clear circles with red border correspond to jejunal samples.

Downloaded from dmd.aspetjournals.org at ASPET Journals on April 19, 2024

DMD Fast Forward. Published on January 20, 2020 as DOI: 10.1124/dmd.119.089656
This article has not been copyedited and formatted. The final version may differ from this version.

Tables

Table 1 Expression levels of enzymes (CYPs and UGTs) with known involvement in drug metabolism in human intestine. Protein expression is represented by the mean, the standard deviation of the mean (SD), the coefficient of variation (%CV) and the range (min – max). Protein abundance is reported in pmol mg^{-1} of total mucosal protein.

	Jejunum (n=4)	***Ileum (n=12)***
	Mean ± SD (%CV) ***Range (min – max)***	***Mean ± SD (%CV)*** ***Range (min – max)***
CYP2C9	1.52 ± 0.61 (40.32)	1.42 ± 0.60 (42.11)
	(0.81 – 2.17)	(0.92 – 3.04)
CYP2C19	1.08 ± 0.11 (10.16)	1.25 ± 0.60 (47.78)
	(0.99 – 1.23)	(0.79 – 3.04)
CYP2D6	1.91 ± 0.46 (23.90)	1.64 ± 0.55 (33.54)
	(1.31 – 2.30)	(1.00 – 2.63)
CYP2J2	1.04 ± 0.30 (28.52)	0.90 ± 0.16 (17.90)
	(0.72 – 1.43)	(0.62 – 1.11)
CYP3A4	33.33 ± 5.70 (17.11)	22.04 ± 10.60 (48.10)
	(24.80 – 36.75)	(7.58 – 34.70)
UGT1A1	2.93 ± 2.17 (73.83)	1.52 ± 0.55 (36.50)
	(0.83 – 5.35)	(0.72 – 2.58)
UGT1A3	1.26 ± 0.29 (22.64)	1.10 ± 0.23 (20.50)
	(0.87 – 1.54)	(0.90 – 1.69)
UGT1A6	0.75 ± 0.02 (2.12)	0.75 ± 0.02 (3.25)
	(0.74 – 0.77)	(0.71 – 0.79)
UGT2B7	1.84 ± 0.97 (53.07)	1.17 ± 0.23 (19.34)
	(1.03 – 3.03)	(0.88 – 1.65)
UGT2B15	0.39 ± 0.03 (8.37)	0.37 ± 0.03 (9.26)
	(0.34 – 0.41)	(0.32 – 0.44)

Downloaded from dmd.aspetjournals.org at ASPET Journals on April 19, 2024

DMD Fast Forward. Published on January 20, 2020 as DOI: 10.1124/dmd.119.089656
This article has not been copyedited and formatted. The final version may differ from this version.

Table 2 Expression levels of one plasma membrane marker (Na/K ATPase), one cell adhesion protein (cadherin-17) and drug transporters with known involvement in drug clearance in human intestine. Protein expression is represented by the mean, the standard deviation of the mean (SD), the coefficient of variation (%CV) and the range (min – max). Protein abundance is reported in pmol mg^{-1} of total mucosal protein.

Transporter	***Jejunum (n=4)***	***Ileum (n=12)***
	Mean ± SD (%CV) ***Range (min – max)***	***Mean ± SD (%CV)*** ***Range (min – max)***
Na^{+}/K^{+-} ATPase	18.86 ± 4.35 (23.07)	13.46 ± 4.62 (34.32)
	(14.88 – 24.01)	(5.71 – 23.39)
Cadherin-17	21.02 ± 6.25 (29.73)	13.49 ± 4.49 (33.26)
	(15.70 – 28.83)	(7.07 – 23.10)
P-gp	0.74 ± 0.22 (29.50)	0.96 ± 0.56 (58.57)
	(0.54 – 1.05)	(0.25 – 2.05)
MRP2	3.33 ± 0.76 (22.80)	2.66 ± 0.65 (24.49)
	(2.76 – 4.43)	(2.02 – 3.98)
BCRP	0.59 ± 0.27 (45.94)	0.45 ± 0.13 (28.03)
	(0.33 – 0.95)	(0.21 – 0.69)
OST-α	1.91 ± 0.15 (7.62)	2.34 ± 0.58 (24.69)
	(1.80 – 2.12)	(1.62 – 3.39)
OST-β	1.72 ± 0.24 (14.02)	1.88 ± 0.39 (20.50)
	(1.50 – 1.97)	(1.18 – 2.60)
OATP2B1	2.65 ± 1.95 (73.37)	3.71 ± 2.50 (67.49)
	(1.19 – 5.47)	(0.21 – 7.51)
OATP1A2	1.50 ± 0.04 (2.88)	1.59 ± 0.31 (19.40)
	(1.44 – 1.54)	(1.44 – 2.46)

Downloaded from dmd.aspetjournals.org at ASPET Journals on April 19, 2024

Figure 1

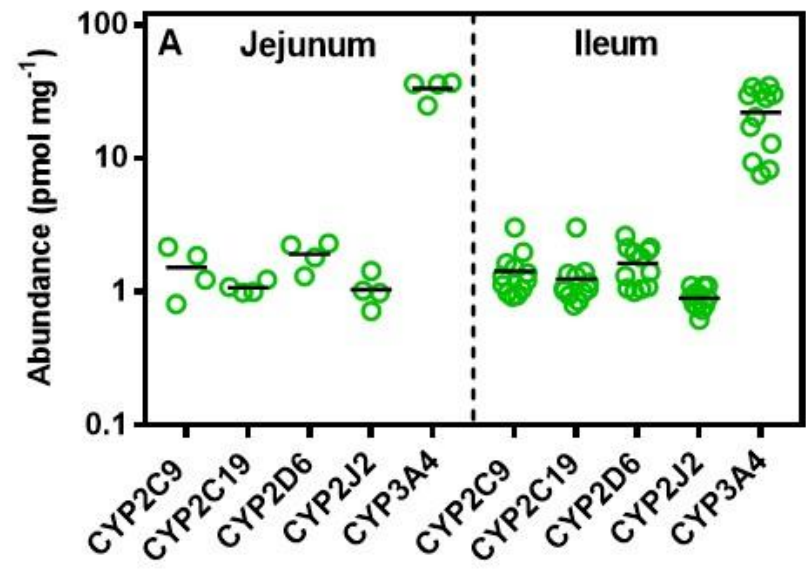

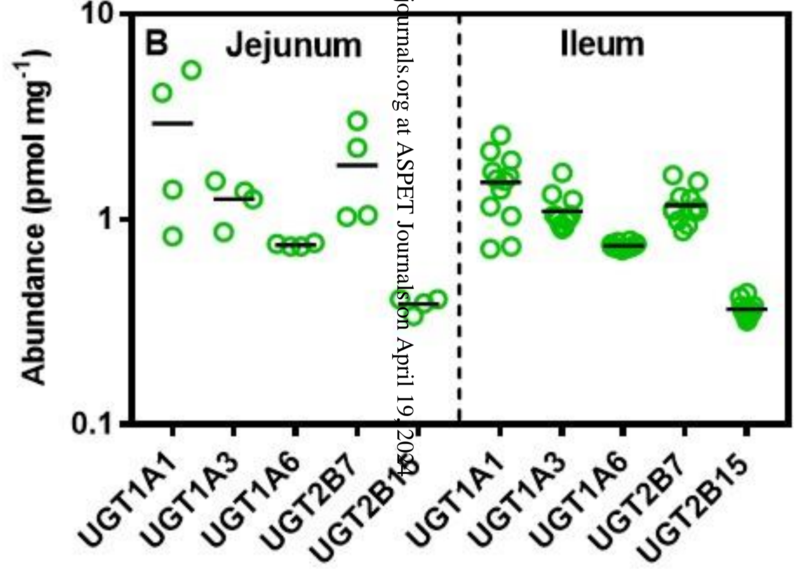

Downloaded from dmd.aspetjournals.org at ASPET Journals on April 19, 2024

Figure 2

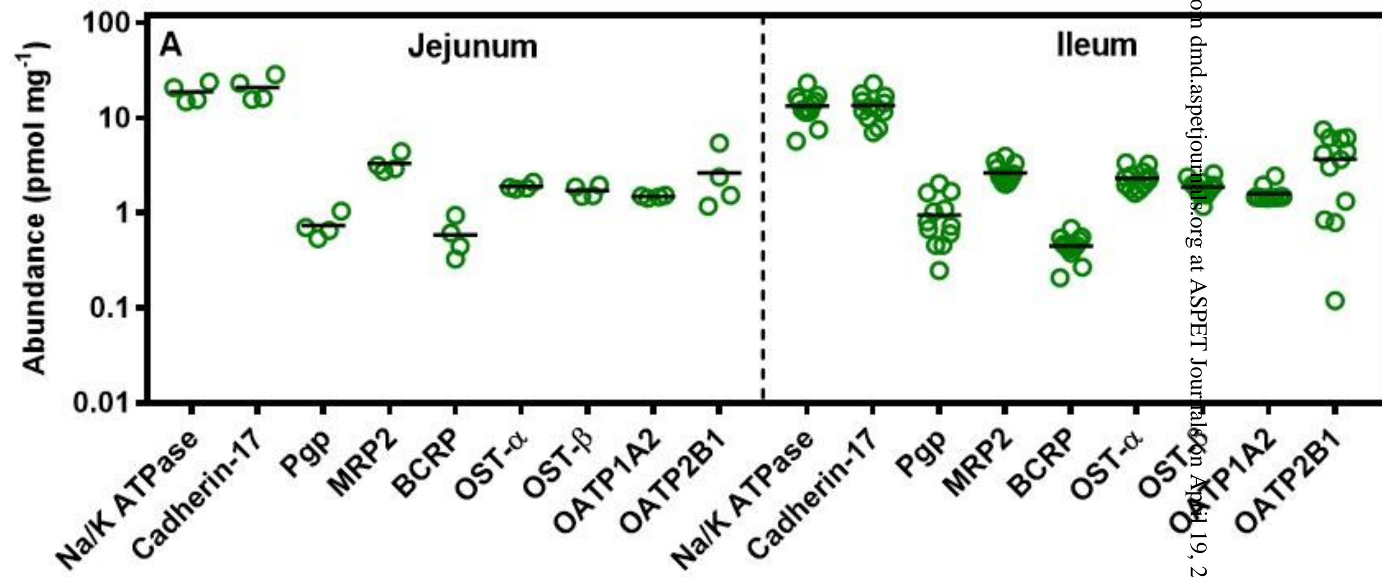

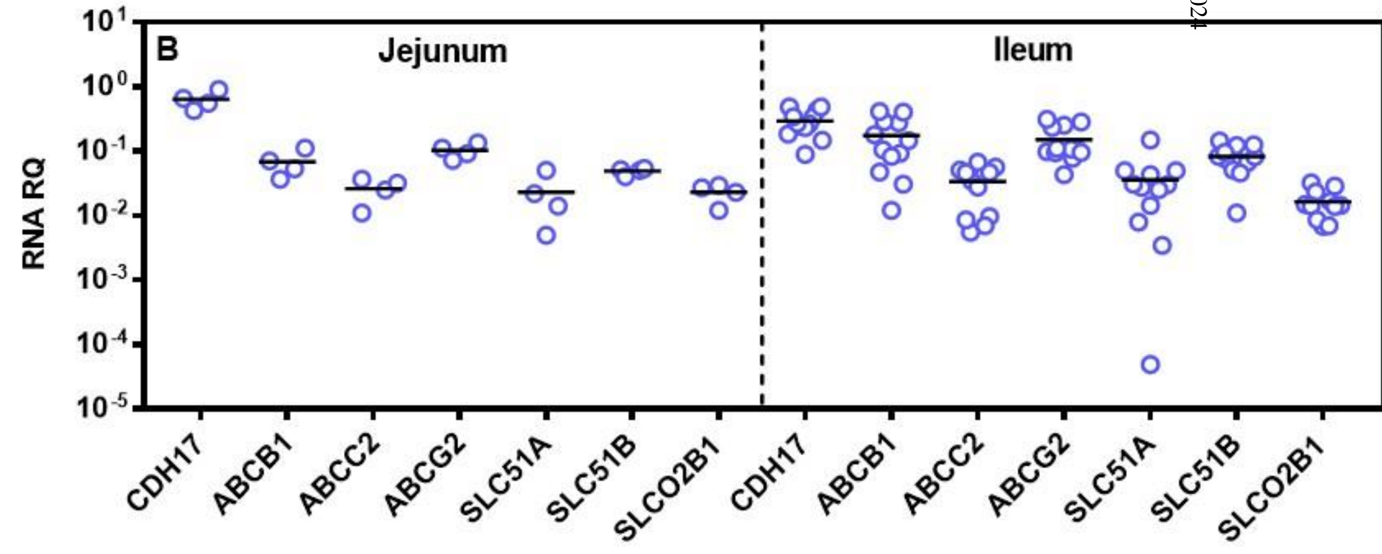

Downloaded from dmd.aspetjournals.org at ASPET Journals on April 19, 2024

Figure 3

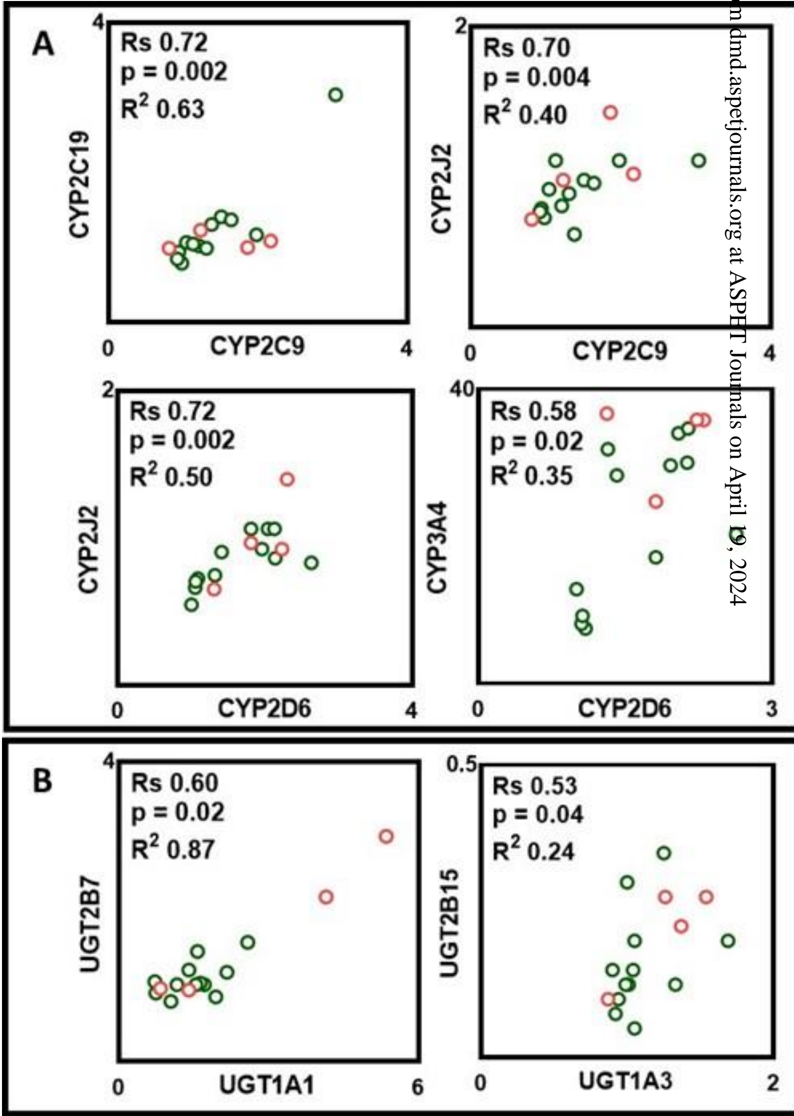

Downloaded from dmd.aspetjournals.org at ASPET Journals on April 19, 2024

Figure 4

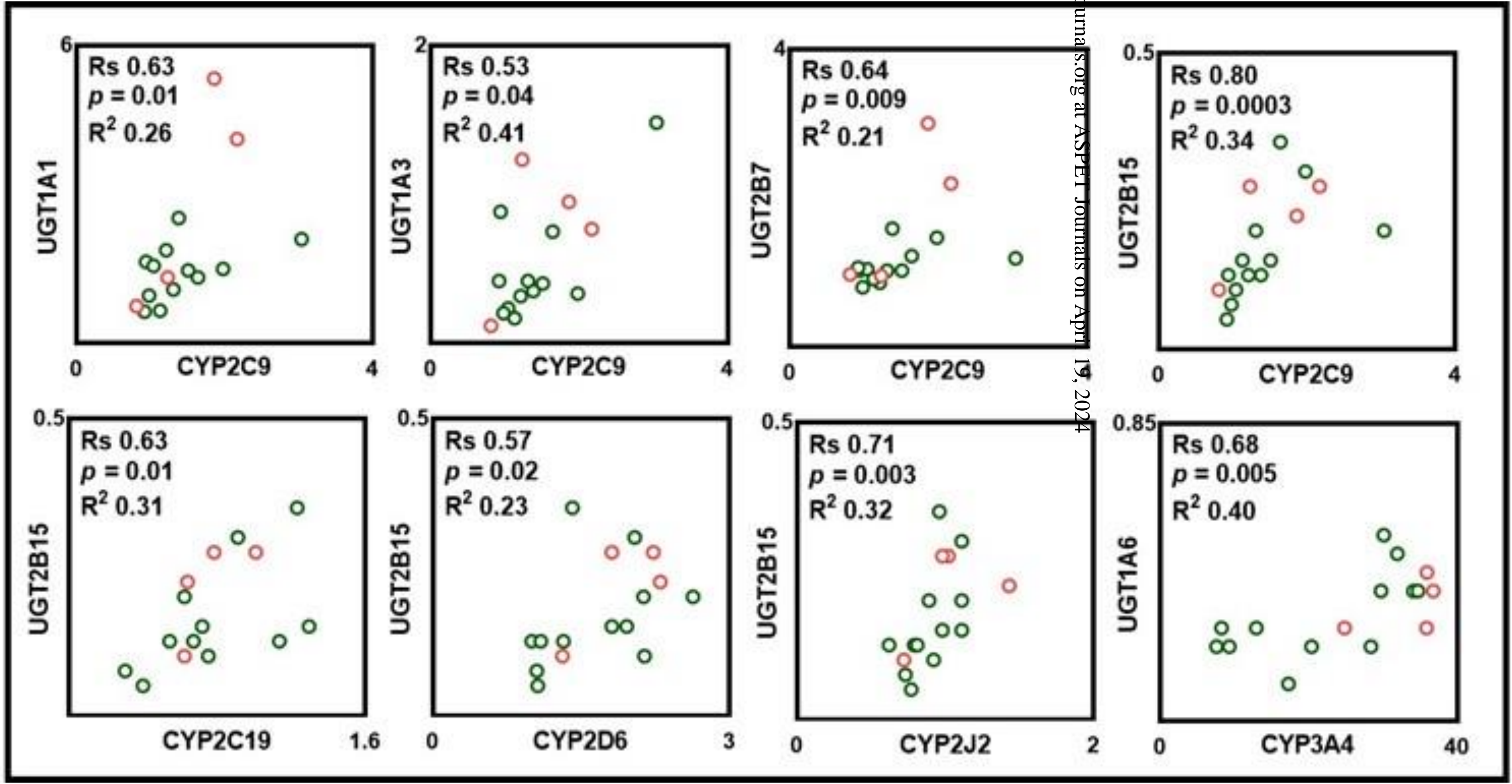

Downloaded from dmd.aspetjournals.org at ASPET Journals on April 19, 2024

Figure 5

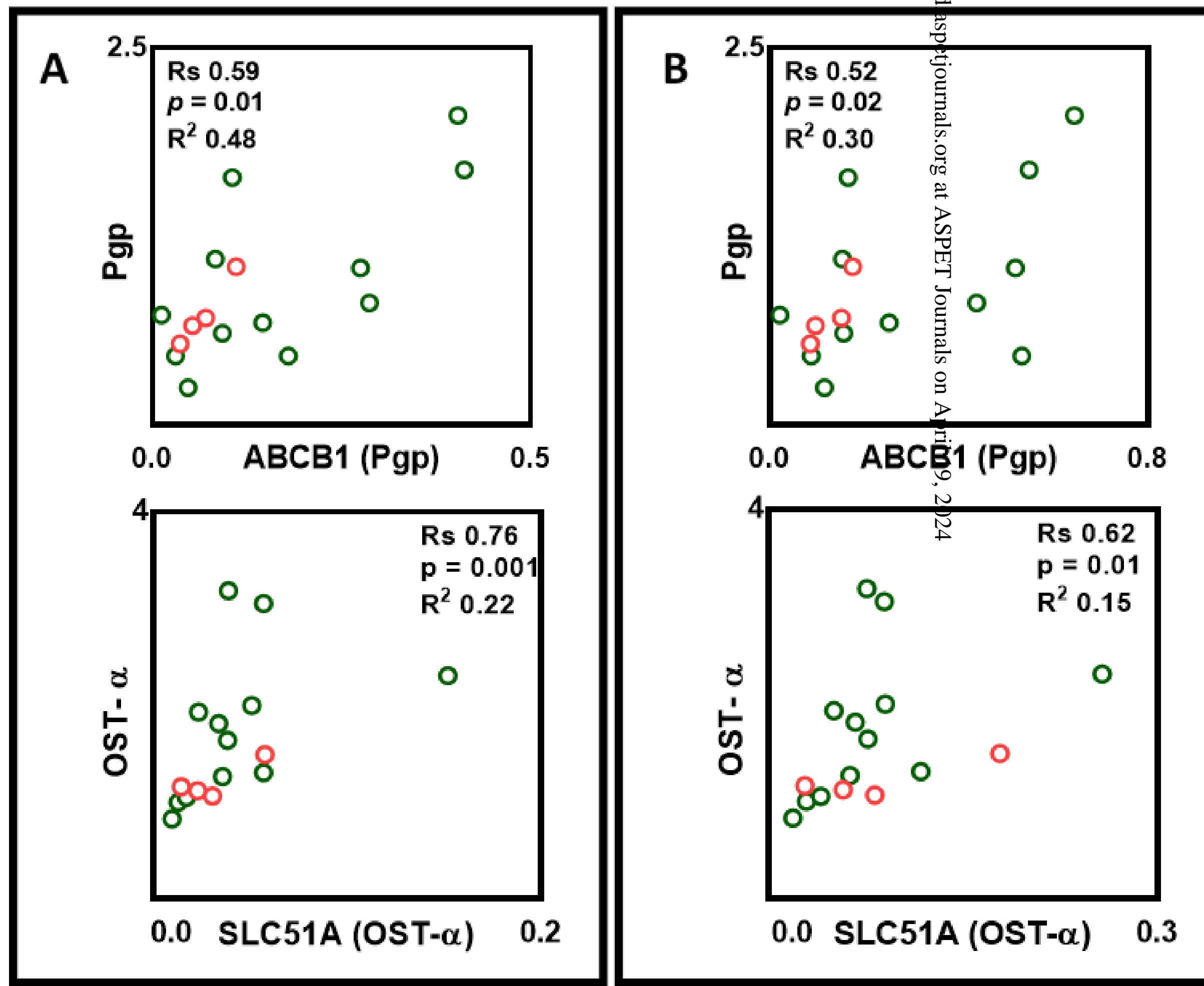

Downloaded from dmd.aspetjournals.org at ASPET Journals on April 9, 2024

Supplementary Information

Quantitative Proteomics of Clinically Relevant Drug-Metabolizing Enzymes and Drug Transporters and Their Inter-correlations in the Human Small Intestine

Narciso Couto[1], Zubida M. Al-Majdoub[1], Stephanie Gibson[2], Pamela J. Davies[2], Brahim Achour[1], Matthew D. Harwood[3], Gordon Carlson[2], Jill Barber[1], Amin Rostami-Hodjegan[1,3], Geoffrey Warhurst[2]

1 Centre for Applied Pharmacokinetic Research, University of Manchester, Stopford Building, Oxford Road, Manchester, M13 9PT, UK.

2 Gut Barrier Group, Inflammation and Repair, University of Manchester, Salford Royal NHS Trust, Salford, M6 8HD, UK

3 Certara UK Limited (Simcyp Division), Level 2 – Acero, 1 Concourse Way, Sheffield, S1 2BJ, UK.

Correspondence to:

Narciso Couto and Amin Rostami-Hodjegan,

Centre for Applied Pharmacokinetic Research, University of Manchester, Stopford Building, Oxford Road, Manchester, M13 9PT, UK

Tel: +44 161 3060634

narciso.couto@manchester.ac.uk, ORCID ID: 0000-0001-7565-4357

amin.rostami@manchester.ac.uk, ORCID ID: 0000-0003-3917-844X

Table 1 – Demographic and clinical details of 28 human intestine samples. Information on age, gender, medical history is provided.

Sample Code	***Tissue Origin***	***Site***	***Sex***	***Age***	***Surgery***	***Disease Classification****	***Medication History***
01	Ileum	Distal Ile	M	80	Right hemicolectomy	Colon cancer	Omeprazole, Codeine phosphate,Paracetamol, Metoclopramide
04	Ileum	Prox Ile	F	65	Resection of fistula	No disease	Omeprazole, Aspirin, Ibuprofen, Simvastatin, Droperidol, Metronidazole, Cefruoxime, Quinine
05	Ileum	Distal Ile	M	28	Crohn's Disease	Inflammatory bowel disease	Loperamide, Codeine phosphate, Paracetamol, Gentamicin, Metronidazole, Cefruoxime
10	Ileum	Prox Ile	M	54	Reversal of stoma - trauma due to previous surgery	No disease	Omeprazole, Oxycodone, Codeine phosphate, Clonidine, Forceval (multivit), Dioralyte
11	Ileum	Distal Ile	M	68	Extended right hemicolectomy	Colon cancer	Lansoprazole, Paracetamol, Chlorphrenamine, Simvastatin, Perindopril, Allopurinol
12	Ileum	Distal Ile	F	78	Crohn's Disease	Inflammatory bowel disease	Omeprazole, Morphine, Tramadol, Codeine phosphate, Paracetamol, Diclofenac, Ibuprofen, Salbutamol, Pravastatin, Azathioprine, Quinine, Tiotropium
15	Jejunum	Mid Jej	M	66	Laparotomy - ischemia	Ischemia	Paracetamol, Atorvastatin, Colestyramine, Glimepiride, Clopidogrel
16	Jejunum	Distal Jej	F	49	Fistula resection	No disease	Lansoprazole, Oxycodone, Fentanyl, Paracetamol, Aspirin, Gabapentin, Salbutamol, Beclomethasone, Prednisolone, Hyoscine
18	Ileum	Distal Ile	F	41	Crohn's Disease	Inflammatory bowel disease	Omeprazole, Codeine phosphate, Paracetamol, Citalopram, Propranolol, Prednisolone
19	Ileum	Distal Ile	M	59	Right hemicolectomy	Colon cancer	Codeine phosphate, Paracetamol, Aspirin, Atorvastatin, Perindopril
20	Ileum	Distal Ile	M	62	Right hemi hepatectomy / total colectomy with ileostomy	Colon cancer	Co-codamol, Salbutamol, Seretide, Glucosamide, Zopiclone, Carbocysteine, Movicol (laxative), St John's Wort
21	Ileum	Prox Ile	M	17	Resection of multiple subcutaneous fistulas	No disease	Omeprazole, Loperamide, Oxycodone, Citalopram, Piriton
22	Jejunum	Prox Jej	M	61	Closure of double barrelled jejunostomy	No disease	Omeprazole, Loperamide, Ferrous fumarate, Forceval (multivit), Ensure, Dioralyte, Magnasparate, Zinc sulphate
23	Jejunum	Prox Jej	M	29	Fistula following ischemia	Ischemia	Ranitidine, Loperamide, Codeine phosphate
26	Ileum	Distal Ile	M	56	Closure of loop colostomy	Colon cancer	No medication
28	Ileum	Distal Ile	M	74	Ileocolic reanastomomosis	Ischemia	Loperamide, Codeine phosphate, Paracetamol

* Disease Classification: indicates any underlying disease present at time of surgery, however in all cases the tissue sample was taken from the healthy margins of the resected tissue and was macroscopically normal. Ile, ileum; Jej, jejunum; Prox, proximal; mid, middle; F, female; M, male.

Table 2 – Overview of the transition schedules and the respective ions selected for the native and isotope labelled peptides used for quantification of drug-metabolising enzymes. The MetCAT construct yields standard peptides labelled with $^{13}C_6$ on the C-terminal arginine (R) or lysine (K) residues. Peptides highlighted in grey were not suitable for quantification and hence not used.

Protein	Peptide	Native/Standard	Q1 (m/z)	Charge	Ion	Q3.1 (m/z)	Ion	Q3.2 (m/z)	Ion	Q3.3 (m/z)
CYP3A4	LSLGGLLQPEKPVVLK	Native	564.35	3	y6	683.48	y5	555.39	y4	458.33
		Standard	566.36	3	y6	689.50	y5	561.41	y4	464.35
CYP3A4	LSLGGLLQPEK	Native	577.84	2	y5	614.35	y4	501.27	y3	373.21
		Standard	580.85	2	y5	620.37	y4	507.29	y3	379.23
CYP3A4	EVTNFLR	Native	439.74	2	y5	650.36	y4	549.31	y3	435.27
		Standard	442.75	2	y5	656.38	y4	555.33	y3	441.29
CYP2C9	LPPGPTPLPVIGNILQIGIK	Native	679.75	3	y9	955.59	y6	671.45	y5	558.36
		Standard	681.76	3	y9	961.61	y6	677.47	y5	564.38
CYP2C9	GIFPLAER	Native	451.76	2	y6	732.40	y5	585.34	y4	488.28
		Standard	454.77	2	y6	738.42	y5	591.36	y4	494.30
CYP2C19	GHFPLAER	Native	463.75	2	y6	732.40	y5	585.34	y4	488.28
		Standard	466.76	2	y6	738.42	y5	591.36	y4	494.30
CYP2C19	IYGPVFTLYFGLER	Native	558.97	3	y6	784.40	y5	621.34	y4	474.27
		Standard	560.97	3	y6	790.42	y5	627.36	y4	480.29
CYP2D6	DIEVQGFR	Native	482.25	2	y6	735.38	y5	606.34	y4	507.27
		Standard	485.26	2	y6	741.40	y5	612.36	y4	513.29
CYP2D6	AFLTQLDELLTEHR	Native	562.63	3	y6	768.44	y5	655.35	y4	542.27
		Standard	564.64	3	y6	774.46	y5	661.37	y4	548.29
CYP2J2	VIGQGQQPSTAAR	Native	656.85	2	y9	915.46	y7	730.38	y6	602.33
		Standard	659.86	2	y9	921.48	y7	736.40	y6	608.35
CYP2J2	FEYQDSWFQQLLK	Native	577.95	3	y6	776.47	y5	629.40	y4	501.34
		Standard	579.96	3	y6	782.49	y5	635.42	y4	507.36
UGT1A1	DGAFYTLK	Native	457.73	2	y5	671.38	y4	524.31	y3	361.24
		Standard	460.74	2	y5	677.40	y4	530.33	y3	367.26
UGT1A1	TYPVPFQR	Native	504.27	2	y6	743.42	y5	646.37	y4	547.30
		Standard	507.28	2	y6	749.44	y5	652.39	y4	553.32

UGT1A3	YLSIPTVFFLR	Native	678.39	2	y7	879.51	y6	782.46	y4	582.34
		Standard	681.40	2	y7	885.53	y6	788.48	y4	588.36
UGT1A6	VSVWLLR	Native	436.77	2	y6	773.47	y5	686.43	y4	587.37
		Standard	439.78	2	y6	779.49	y5	692.45	y4	593.39
UGT1A6	SFLTAPQTEYR	Native	656.83	2	y7	864.42	y6	793.38	y4	568.27
		Standard	659.84	2	y7	870.44	y6	799.40	y4	574.29
UGT2B7	ADVWLIR	Native	436.75	2	y6	801.46	y4	587.37	y3	401.29
		Standard	439.76	2	y6	807.48	y4	593.39	y3	407.31
UGT2B7	TILDELIQR	Native	550.82	2	y7	886.50	y6	773.42	y5	658.39
		Standard	553.83	2	y7	892.52	y6	779.44	y5	664.41
UGT2B15	SVINDPVYK	Native	517.78	2	y7	848.45	y6	735.37	y5	506.30
		Standard	520.79	2	y7	854.47	y6	741.39	y5	512.32
UGT2B15	WIYGVSK	Native	426.73	2	y6	666.38	y5	553.30	y4	390.23
		Standard	429.74	2	y6	672.40	y5	559.32	y4	396.25
Mod-GluFib	GVNDNEEGFFSAR	Native	721.32	2	y8	942.43	y7	813.39	y6	684.35
		Standard	724.33	2	y8	948.45	y7	819.41	y6	690.37

Table 3 – Overview of the transition schedules and the respective ions selected for the native and isotope labelled peptides used for quantification of transporters. The TransCAT construct yields standard peptides labelled with $^{13}C_6$ on the C-terminal arginine (R) or lysine (K) residues. Peptides highlighted in grey were not suitable for quantification and hence not used.

Protein	Peptide	Native/Standard	Q1 (m/z)	Charge	Ion	Q3.1 (m/z)	Ion	Q3.2 (m/z)	Ion	Q3.3 (m/z)
Na^+/K^+-ATPase	IVEIPFNSTNK	Native	631.34	2	y8	920.48	y7	807.40	y4	449.24
		Standard	634.35	2	y8	926.50	y7	813.42	y4	455.26
Na^+/K^+-ATPase	NPNTSEPQHLLVMK	Native	536.61	3	y6	740.45	y5	603.39	y4	490.31
		Standard	538.62	3	y6	746.47	y5	609.41	y4	496.33
HPT1	AENPEPLVFGVK	Native	650.35	2	y9	985.57	y7	759.48	y4	450.27
		Standard	653.36	2	y9	991.59	y7	765.50	y4	456.29
HPT1	DEENTANSFLNYR	Native	524.90	3	+3y5	712.38	+3y4	565.31	+3y3	452.23
		Standard	526.91	3	+3y5	718.40	+3y4	571.33	+3y3	458.25
Pgp	AGAVAEEVLAAIR	Native	635.36	2	y9	971.55	y8	900.51	y7	771.47
		Standard	638.37	2	y9	977.57	y8	906.54	y7	777.49
Pgp	EANIHAFIESLPNK	Native	528.28	2	y6	687.37	y5	558.32	y3	358.21
		Standard	530.29	2	y6	693.39	y5	564.34	y3	364.23
MRP2	LVNDIFTFVSPQLLK	Native	578.67	3	y7	784.49	y6	685.42	y5	598.39
		Standard	580.67	3	y7	790.51	y6	691.44	y5	604.41
MRP2	LLISFASDR	Native	511.29	2	y7	795.40	y6	682.32	y5	595.28
		Standard	514.30	2	y7	801.42	y6	688.34	y5	601.30
BCRP	VIQELGLDK	Native	507.80	2	y7	802.43	y6	674.37	y4	432.25
		Standard	510.81	2	y7	808.45	y6	680.39	y4	438.27
BCRP	TIIFSIHQPR	Native	404.57	3	y6	737.41	y5	650.37	y4	537.29
		Standard	406.57	3	y6	743.43	y5	656.39	y4	543.31
OST-α	YTADLLEVLK	Native	582.83	2	y8	900.54	y7	829.50	y6	714.48
		Standard	585.84	2	y8	906.56	y7	835.52	y6	720.50
OST-β	ETPEVLHLDEAK	Native	460.91	3	y6	712.36	y5	575.30	y4	462.22
		Standard	462.91	3	y6	718.38	y5	581.32	y4	468.24
OST-β	DHNSLNNLR	Native	541.77	2	y7	830.45	y6	716.40	y5	629.37

		Standard	544.78	2	y7	836.47	y6	722.43	y5	635.39
OATP2B1	ATMGTENTPGGK	Native	582.27	2	y10	991.45	y9	860.41	y4	358.21
		Standard	585.28	2	y10	997.47	y9	866.43	y4	364.23
OATP2B1	TGSVICFALVLAVLR	Native	540.32	3	y6	670.46	y5	571.39	y4	458.31
		Standard	542.32	3	y6	676.48	y5	577.41	y4	464.33
OATP1A2	EGLETNADIIK	Native	601.82	2	y8	903.48	y7	774.44	y6	673.39
		Standard	604.83	2	y8	909.50	y7	780.46	y6	679.41
OATP1A2	IYDSTTFR	Native	501.75	2	y7	889.41	y6	726.34	y5	611.31
		Standard	504.76	2	y7	895.43	y6	732.36	y5	617.33
Glu-Fib	EGVNDNEEGFFSAR	Native	785.84	2	y8	942.43	y7	813.39	y6	684.35
		Standard	788.85	2	y8	948.45	y7	819.41	y6	690.37

Table 4 – Real time PCR primers (forward and reverse) for human intestinal transporters.

Gene Symbol	*Forward Primer Sequence (5' – 3')*	*Reverse Primer Sequence (5' – 3')*	*Universal ProbeLibrary (UPL) number*
VIL1	TTGCCACAATTCCCTGAGAT	CTTGGTCATGGTGAGTGAGC	87
GAPDH	AGCCACATCGCTCAGACAC	GCCCAATACGACCAAATCC	60
CDH-17	CGTCACCAGTAACCGTATTTGA	GTGCAGTAAGGGTCCCGATA	2
ABCB1	CGGAGTATCTTCTTCCAAGATTTC	TCCCCTTCAAGATCCATCC	49
ABCC2	AGTGAATGACATCTTCACGTTTG	CTTGCAAAGGAGATCAGCAA	73
ABCG2	TGGCTTAGACTCAAGCACAGC	TCGTCCCTGCTTAGACATCC	56
SLC51A	CTGAAGACCAATTACGGCATC	GAGGGCAAGTTCCACAGG	75
SLC51B	AGCATCCAGGCAAGCAGA	CCTCATCCAAATGCAGGACT	83
SLCO2B1	GATCCTGTTTGCAGTGACCA	CCTTTATGGTCAGGCTGATACC	23

Table 5 – Comparison of the abundance of drug-metabolising enzymes quantified in the present study with data reported in the literature.

	*(Harbourt et al., 2012)**	*(Sato et al., 2014)***	*(Miyauchi et al., 2016)****	*(Akazawa et al., 2018)¥*		*(Drozdzik et al., 2019)¥¥*		*The present work¥¥¥*	
			Jejunum	Jejunum	Ileum	Jejunum	Ileum	Jejunum	Ileum
CYP2C9			3.15 ± 1.25 (n=28)	0.51 ± 0.09 3.74 ± 0.25	0.72 ± 0.08 3.23 ±0.08	0.034 ± 0.023 (n=18)	0.009 ± 0.004 (n=9)	1.52 ± 0.61 (40.32)	1.42 ± 0.60 (42.11)
CYP2C18				BLQ 1.50 ± 0.11	BLQ				
CYP2C19			0.43 ± 0.17 (n=26)			0.003 ± 0.003 (n=9)	BLQ	1.08 ± 0.11 (10.16)	1.25 ± 0.60 (47.78)
CYP2D6			1.87 ± 1.11 (n=27)	BLQ 1.18 ± 0.10	BLQ 1.16 ± 0.05	0.004 ± 0.003 (n=11)	0.003 ± 0.004 (n=4)	1.91 ± 0.46 (23.90)	1.64 ± 0.55 (33.54)
CYP2J2			0.37 ± 0.18 (n=28)	- 5.28 ± 0.42	2.71 ± 0.77 5.55 ± 0.46			1.04 ± 0.30 (28.52)	0.90 ± 0.16 (17.90)
CYP3A4			23.4 ± 8.4 (n=28)	6.20 ± 0.36 9.84 ± 0.43	8.03 ± 0.40 12.9 ± 0.50	0.135 ± 0.134 (n=18)	0.092 ± 0.126 (n=9)	33.33 ± 5.70 (17.11)	22.04 ± 10.60 (58.10)
CYP4A11				BLQ 0.25 ± 0.01	BLQ 0.13 ± 0.01				
CYP51A1				0.72 ± 0.05 1.33 ± 0.09	0.72 ± 0.05 1.07 ± 0.09				
UGT1A1	7.2 ± 3.7 (51.3)	39.6 ± 21.4 (54.1)	11.0 ± 3.3 (n=28)	BLQ 4.57 ± 0.22	BLQ 5.05 ± 0.38	0.101 ± 0.068 (n=18)	0.036 ± 0.021 (n=8)	2.93 ± 2.17 (73.83)	1.52 ± 0.55 (36.50)
UGT1A3	BLD	1.93 ± 1.10 (56.9)	0.84 ± 0.31 (n=28)			0.002 ± 0.003 (n=5)	BLQ	1.26 ± 0.29 (22.64)	1.10 ± 0.23 (20.50)
UGT1A4	5.3 ± 0.7 (13.4)	1.60 ± 0.90 (56.5)	0.55 ± 0.34 (n=21)						
UGT1A6	2.3 ± 1.2 (49.8)	ND	1.69 ± 0.71 (n=28)	BLQ 1.76 ± 0.17	BLQ 1.54 ± 0.10			0.75 ± 0.02 (2.12)	0.75 ± 0.02 (3.25)
UGT1A7	8.4 ± 2.4 (28.0)								
UGT1A8	6.1 ± 3.8 (62.8)								
UGT1A9	6.6 ± 1.4 (21.7)								
UGT1A10	4.7 ± 2.8 (59.3)								
UGT2B7		15.7 ± 9.81 (62.6)	4.22 ± 1.35 (n=28)	BLQ 5.29 ± 0.98	BLQ 5.59 ± 0.63	0.023 ± 0.012 (n=18)	0.006 ± 0.004 (n=8)	1.84 ± 0.97 (53.07)	1.17 ± 0.23 (19.34)

UGT2B15		ND	25.2 (n=1)					0.39 ± 0.03 (8.37)	0.37 ± 0.03 (9.26)
UGT2B17		36.6 ± 32.7 (72.8)		4.91 ± 0.12 7.63 ± 2.30	7.63 ± 0.32 33.7 ± 1.30				

* Results expressed as pmol mg^{-1} protein from 3 human intestinal samples analysed in duplicate (mean ± SD (%CV)). ** Results expressed as pmol mg^{-1} protein from 6 male intestinal samples (mean ± SD (%CV)). *** Results expressed as pmol mg^{-1} of microsomal proteins in jejunal samples from morbidly obese individuals (mean ± SD (n = number of samples)). ¥ Results expressed as pmol mg^{-1} protein from 2 independent human intestinal samples analysed in triplicate (mean ± SEM). ¥¥ Results expressed as pmol mg^{-1} intestinal tissue from 9 samples (mean ± SD (number of samples)). ¥¥¥In the present study, protein abundances are expressed as pmol mg^{-1} protein from human intestinal samples analysed in duplicate (mean ± SD (%CV)). ND not determined. BLQ represents below the limit of quantification.

Table 6 – Comparison of the abundance of drug transporters quantified in the present study with data reported in the literature.

	*(Gröer et al., 2013)**		*(Drozdzik et al., 2014) ***		*(Miyauchi et al., 2016)****	*(Harwood et al., 2015, 2016)[¥]*		*(Drozdzik et al., 2019)[§]*		*The present work*	
	Jejunum (1 donor, 6 technical replicates)	Ileum (3 donors, 3 biological replicates)	Jejunum (6 donors)	Ileum (6 donors)	Jejunum (24 donors)	Jejunum (3 donors)	Ileum (1 donor)	Jejunum (6 donors)	Ileum (6 donors)	Jejunum	Ileum
Na/K ATPase					179.0 ± 33.0	35.4 ± 6.2[¥¥] 39.3 ± 3.5[¥¥¥]	24.47[¥¥] 50.72[¥¥¥]			18.86 ± 4.35 (23.07)	13.46 ± 4.62 (34.32)
Cadherin-17						7.4 ± 3.1[¥¥]	6.93[¥¥]			21.02 ± 6.25 (29.73)	13.49 ± 4.49 (33.26)
Pgp	0.61 ± 0.04	0.64 ± 0.10	0.41 ± 0.14 0.48 ± 0.19	0.72 ± 0.31 1.06 ± 0.50	1.22 ± 0.37	1.9 ± 1.1[¥¥] 0.8 ± 0.3[¥¥¥]	0.20[¥¥] BLQ[¥¥¥]	40.21 ± 18.67 (46.42)	70.78 ± 35.47 (50.15)	0.74 ± 0.22 (29.50)	0.96 ± 0.56 (58.57)
BCRP	0.57 ± 0.04	0.69 ± 0.07	0.28 ± 0.19 0.36 ± 0.19	0.40 ± 0.29 0.36 ± 0.18	1.25 ± 0.54	2.6 ± 0.8[¥¥] 2.1 ± 1.1[¥¥¥]	1.6[¥¥] 0.44[¥¥¥]	23.27 ± 8.96 (38.50)	30.47 ± 11.04 (36.22)	0.59 ± 0.27 (45.94)	0.45 ± 0.13 (28.03)
MRP2	1.06 ± 0.16	0.35 ± 0.07	1.04 ± 0.64 0.95 ± 0.52	0.76 ± 0.50 0.82 ± 0.48	0.12 ± 0.04	0.6 ± 0.2[¥¥]	BLQ[¥¥]	22.44 ± 9.86 (43.13)	19.84 ± 7.18 (36.18)	3.33 ± 0.76 (22.80)	2.66 ± 0.65 (24.49)
OST-α					4.45 ± 1.35	0.5 ± 0.2[¥¥]	0.28[¥¥]			1.91 ± 0.15 (7.62)	2.34 ± 0.58 (24.69)
OS-β					3.87 ± 1.02					1.72 ± 0.24 (14.02)	1.88 ± 0.39 (20.50)
OATP2B1	0.30 ± 0.04	0.25 ± 0.05	0.59 ± 0.32 0.49 ± 0.32	0.46 ± 0.28 0.49 ± 0.21	0.54 ± 0.13			7.61 ± 1.78 (23.42)	8.06 ± 1.87 (23.15)	2.65 ± 1.95 (73.37)	3.71 ± 2.50 (67.49)
OATP1A2										1.50 ± 0.04 (2.88)	1.59 ± 0.31 (19.40)

* Results expressed as pmol mg^{-1} membrane protein. Results are presented as mean ± SD. ** Results expressed as pmol mg^{-1} membrane protein. Results are presented as mean ± SD in two jejunum and ileum regions. *** Results expressed as pmol mg^{-1} of microsomal proteins in jejunal samples from morbidly obese individuals (mean ± SD). ¥ Results expressed as pmol mg^{-1} membrane protein. [¥¥] Results from the University of Manchester. [¥¥¥] Results from Bertin Pharma on matched samples. [§] Results expressed as pmol mg^{-1} intestinal tissue (mean ± SD (%CV)). BLQ represents below the limit of quantification. In the present study, protein abundances are expressed as pmol mg^{-1} protein from human intestinal samples analysed in duplicate (mean ± SD (%CV)).

Figure 1 – Experimental workflow. QconCAT technology was applied to quantify cytochrome P450 (CYP), uridine 5'-diphospho-glucuronosyltransferase (UGT) and transporters in 16 human intestine (HI) crude membrane samples. Each sample was digestion was performed by Lys-C/trypsin digestion using filter aided sample preparation (FASP). After digestion, peptides were desalted using C18 columns. Peptides were reversed-phase separated on an LC system. Eluted peptides were then targeted using a mass spectrometer. Transitions were acquired for targeted peptides. Skyline was used to extract quantification information of the proteins of interest. MRM, multiple reaction monitoring; QconCAT, quantification concatemer; RP-UHPLC, reversed-phase ultra-high performance liquid chromatography.

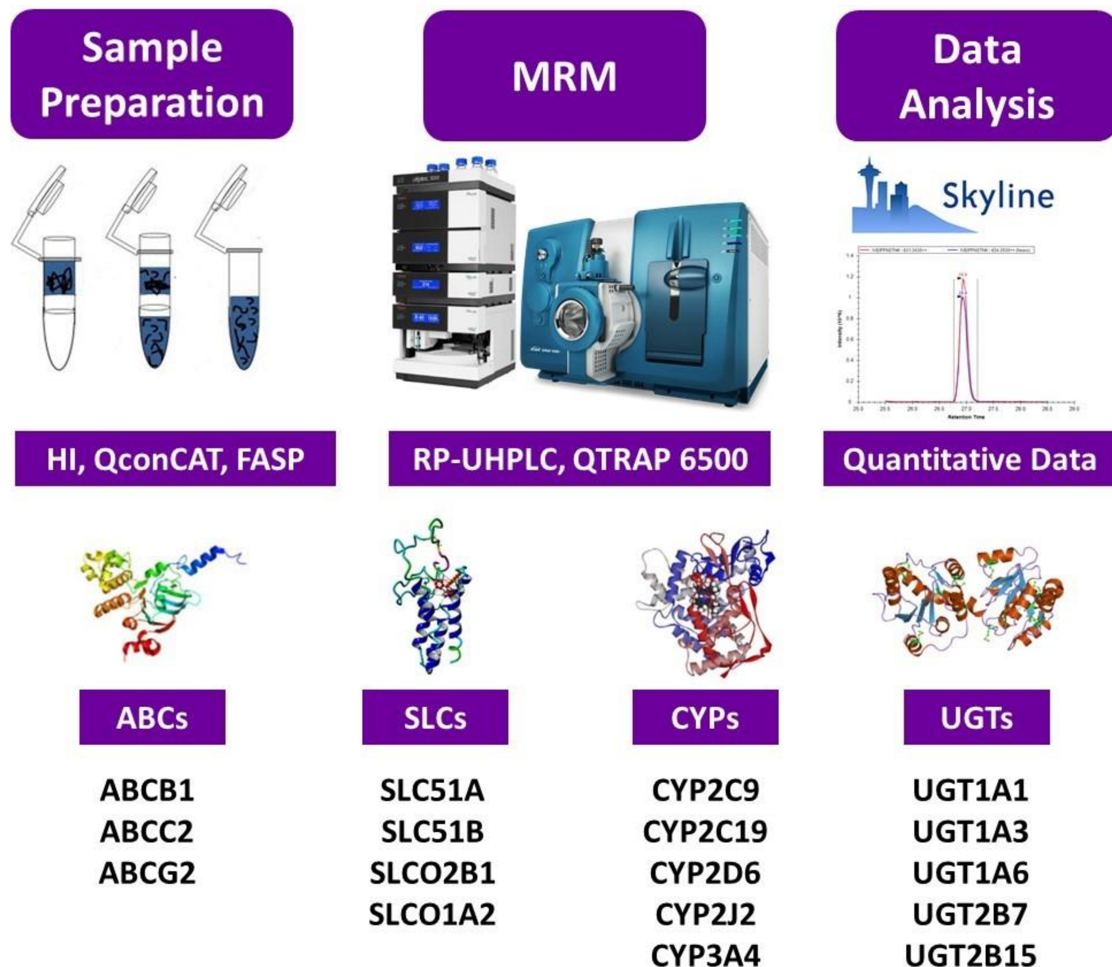

Figure 2 – Representative examples of co-elution profiles of selected ABC transporters, the membrane marker (Na^{+}/K^{+} ATPase) and HPT1, a cell-cell adhesion molecule which also functions as a proton-dependent oligopeptide transporter in the GI tract. Profiles were captured using Skyline. A. The cumulative profiles of the 3 product transitions selected for the native (red) and standard (blue) peptide. B. The peak profiles for the 3 selected transitions for the standard peptide. C. The peak profiles for the 3 selected transitions for the native peptide. Retention time (RT) is represented on the x-axis.

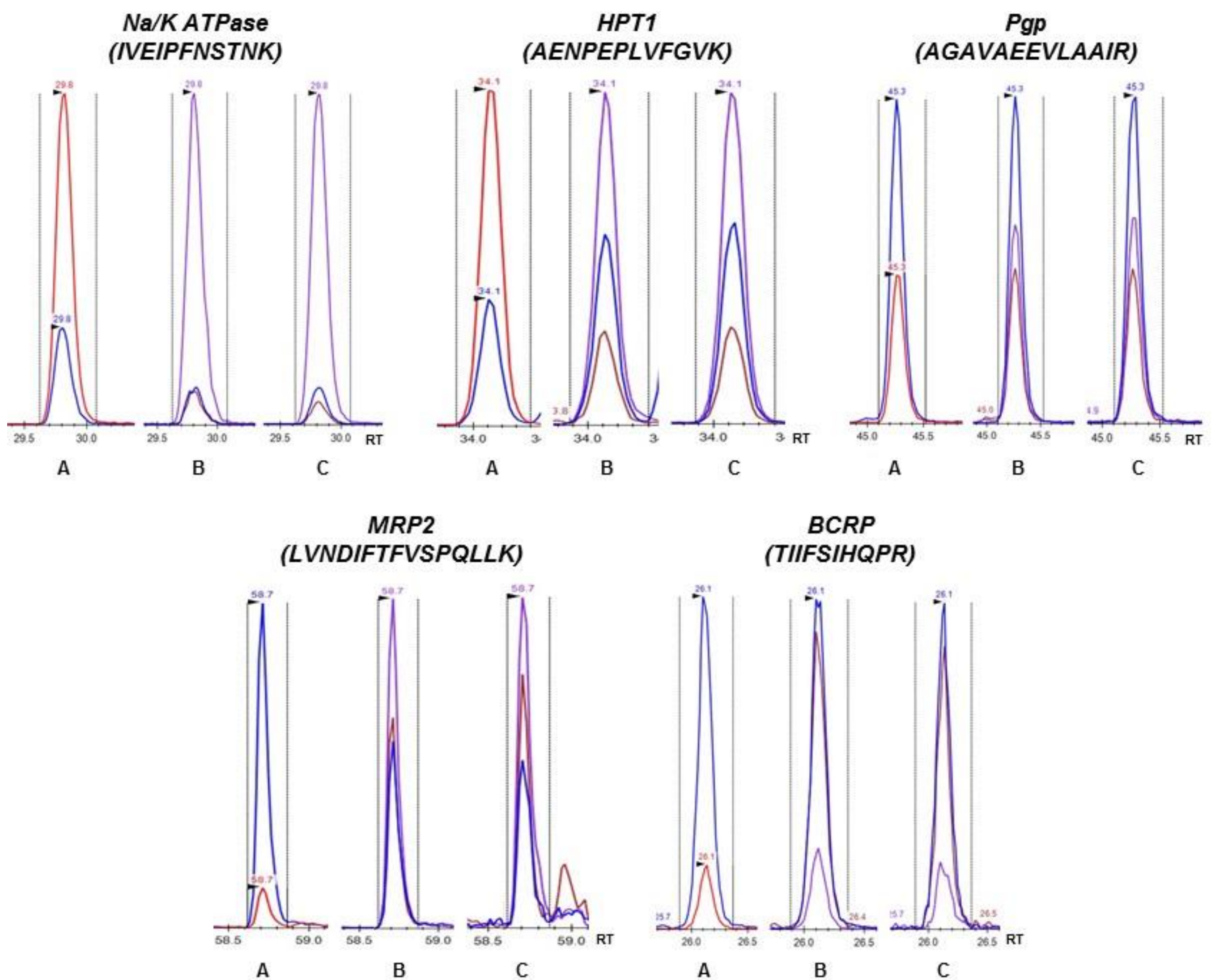

Figure 3 – Representative examples of co-elution profiles of selected SLC transporters. Profiles were captured using Skyline. A. The cumulative profiles of the 3 product transitions selected for the native (red) and standard (blue) peptide. B. The peak profiles for the 3 selected transitions for the standard peptide (except for OATP2B1 where two transitions were used). C. The peak profiles for the 3 selected transitions for the native peptide (except for OATP2B1 where two transitions were used). Retention time (RT) is represented on the x-axis.

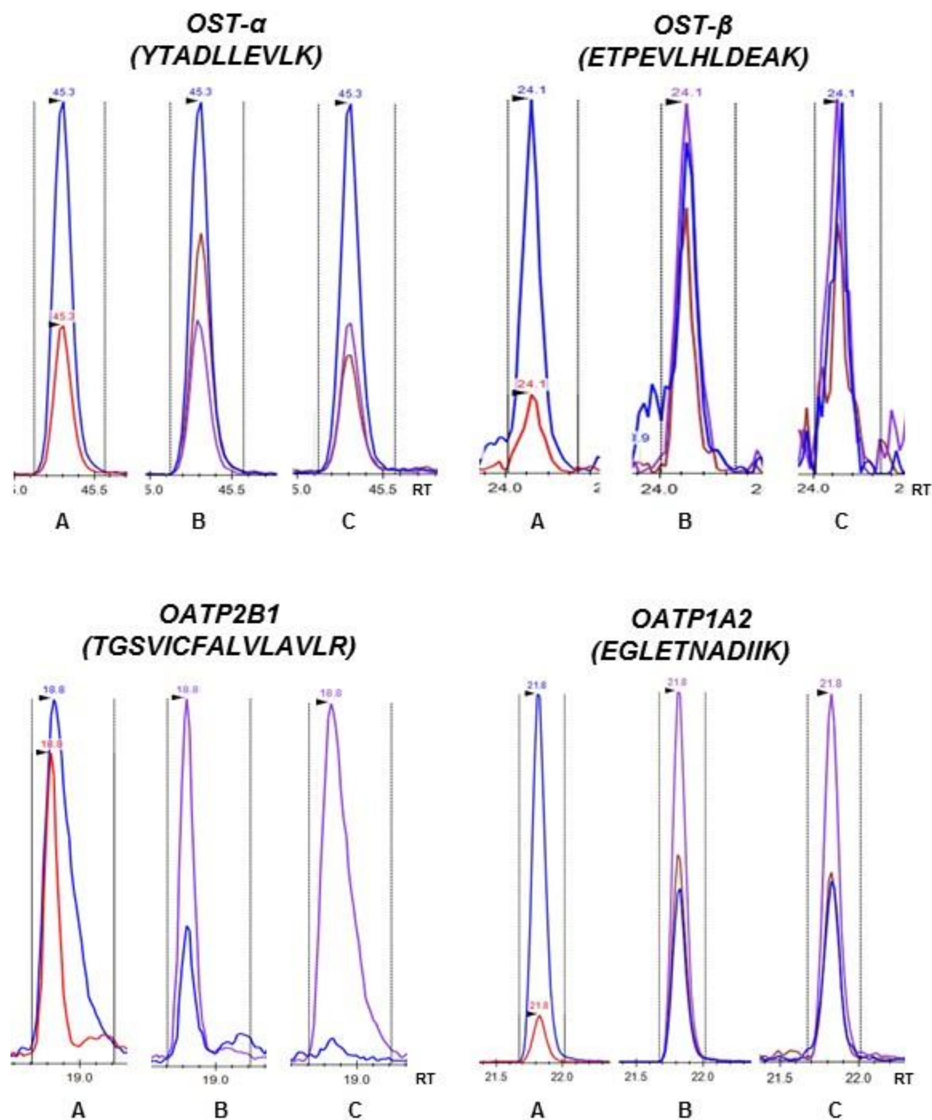

References

Akazawa T, Uchida Y, Miyauchi E, Tachikawa M, Ohtsuki S, and Terasaki T (2018) High Expression of UGT1A1/1A6 in Monkey Small Intestine: Comparison of Protein Expression Levels of Cytochromes P450, UDP-Glucuronosyltransferases, and Transporters in Small Intestine of Cynomolgus Monkey and Human. *Mol Pharm* **15**:127–140.

Drozdzik M, Busch D, Lapczuk J, Müller J, Ostrowski M, Kurzawski M, and Oswald S (2019) Protein Abundance of Clinically Relevant Drug Transporters in the Human Liver and Intestine: A Comparative Analysis in Paired Tissue Specimens. *Clin Pharmacol Ther* **105**:1204–1212.

Drozdzik M, Gröer C, Penski J, Lapczuk J, Ostrowski M, Lai Y, Prasad B, Unadkat JD, Siegmund W, and Oswald S (2014) Protein Abundance of Clinically Relevant Multidrug Transporters along the Entire Length of the Human Intestine. *Mol Pharm* **11**:3547–3555.

Gröer C, Brück S, Lai Y, Paulick A, Busemann A, Heidecke CD, Siegmund W, and Oswald S (2013) LC–MS/MS-based quantification of clinically relevant intestinal uptake and efflux transporter proteins. *J Pharm Biomed Anal* **85**:253–261.

Harbourt DE, Fallon JK, Ito S, Baba T, Ritter JK, Glish GL, and Smith PC (2012) Quantification of Human Uridine-Diphosphate Glucuronosyl Transferase 1A Isoforms in Liver, Intestine, and Kidney Using Nanobore Liquid Chromatography–Tandem Mass Spectrometry. *Anal Chem* **84**:98–105.

Harwood MD, Achour B, Neuhoff S, Russell MR, Carlson G, and Warhurst G (2016) In Vitro-In Vivo Extrapolation Scaling Factors for Intestinal P-Glycoprotein and Breast Cancer Resistance Protein: Part I: A Cross-Laboratory Comparison of Transporter-Protein Abundances and Relative Expression Factors in Human Intestine and Caco-2 Cells. *Drug Metab Dispos* **44**:297–307.

Harwood MD, Achour B, Russell MR, Carlson GL, Warhurst G, and Rostami-Hodjegan A (2015) Application of an LC-MS/MS method for the simultaneous quantification of human intestinal transporter proteins absolute abundance using a QconCAT technique. *J Pharm Biomed Anal* **110:**27-33.

Miyauchi E, Tachikawa M, Declèves X, Uchida Y, Bouillot J-L, Poitou C, Oppert J-M, Mouly S, Bergmann J-F, Terasaki T, Scherrmann J-M, and Lloret-Linares C (2016) Quantitative Atlas of Cytochrome P450, UDP-Glucuronosyltransferase, and Transporter Proteins in Jejunum of Morbidly Obese Subjects. *Mol Pharm* **13**:2631–2640.

Sato Y, Nagata M, Tetsuka K, Tamura K, Miyashita A, Kawamura A, and Usui T (2014) Optimized Methods for Targeted Peptide-Based Quantification of Human Uridine 5’-Diphosphate-Glucuronosyltransferases in Biological Specimens Using Liquid Chromatography-Tandem Mass Spectrometry. *Drug Metab Dispos* **42**:885–889.